Report on WP PFC SP4: *Modelling in 2020*

A. Kirschner on behalf of SP4

This work has been carried out within the framework of the EUROfusion Consortium and has received funding from the Euratom research and training programme 2014-2018 and 2019-2020 under grant agreement No 633053. The views and opinions expressed herein do not necessarily reflect those of the European Commission.

Acknowledgments

Contributors (main contact persons) to WP PFC SP4 in 2020:

CEA: *G. Ciraolo, Y. Ferro, K. Hassouni, Y. Marandet, A. Michau*

ENEA: *M. Passoni, A. Ucello, E. Vassallo*

FZJ: *A. Eksaeva, D. Matveev, D. Reiser, J. Romazanov*

IPP: *K. Schmid*

IPP.CR: *R. Dejarnac, M. Komm, D. Tskhakaya*

KIT: *Ch. Day, S. Varoutis*

ÖAW: *M. Probst*

VR: *S. Ratynskaia*

VTT: *M. Groth, A. Hakola, K. Nordlund*

Structure of WP PFC SP4

SP4.1 Plasma background and plasma sheath modelling

- *Modelled plasma backgrounds and plasma sheaths for tokamaks and linear devices to be used as input for PFC SP4.2*

SP4.2 Plasma-surface interaction and transport modelling

- *Dedicated plasma-wall interaction and material transport modelling in comparison with experiments, predictions for ITER*
- *Particle-surface interaction (modelling of data for erosion, reflection, mixing, …) and atomic/molecular data*

SP4.4 Plasma background and plasma-wall interaction modelling for WEST

- *Modelling of plasma backgrounds for WEST*
- *Modelling of plasma-surface interaction in WEST*

Distribution of PM (ppy)

	RU	ppy 2014	ppy 2015	ppy 2016	ppy 2017	PM (ppy) 2018	PM 2019	PM 2020
SP4.1	CEA	0.7	0.5	0.2	0.2	2.4 (0.2)	2.5	**2.5**
	FZJ	0.7	0.6	0.6	0.6	7.2 (0.6)	----	----
	IPP	0.2	----	----	----	----	----	----
	ÖAW	0.2	0.3	0.3	0.4	4.8 (0.4)	2.5	----
	IPP.CR	----	----	----	----	----	2.5	**2.0**
	VTT	0.1	0.2	0.2	0.2	2.4 (0.2)	1.0	**1.0**

Distribution of PM (cont´d)

	RU	ppy 2014	ppy 2015	ppy 2016	ppy 2017	PM (ppy) 2018	PM 2019	PM 2020
SP4.2	CEA	----	----	----	0.2	2.4 (0.2)	2.5	**2.5**
	ENEA	0.1	0.0	----	----	----	----	**3.0**
	FZJ	0.6	0.6	0.7	0.7	8.4 (0.7)	32.0	**32.0**
	IPP	0.2	0.2	0.2	0.1	1.2 (0.1)	1.5	**1.5**
	IPPLM	0.3	----	----	----	----	----	**----**
	KIT	----	----	----	----	----	----	**4.0**
	ÖAW	0.1	0.2	0.2	0.2	2.4 (0.2)	2.5	**2.5**
	VTT	0.8	0.8	0.7	0.7	8.4 (0.7)	8.5	**8.5**
SP4.4	CEA	----	0.8	0.9	0.8	7.2 (0.6)	7.0	**19.0**
	IPP.CR	----	----	----	0.3	8.4 (0.7)	6.0	**8.5**
	VR					6.0 (0.5)	8.5	**8.0**
		∑ 4.0	**∑ 4.2**	**∑ 4.0**	**∑ 4.4**	**∑ 61.2 (5.1)**	**∑ 77.0**	**∑ 95.0**

Summary

SubProject	Tasks in 2020		Status
SP4.1	CEA:	- Dust modelling	✓
	IPP.CR:	- PIC sheath modelling	✓
	VTT:	- Plasma background modelling	✓
SP4.2	CEA:	- DFT, diffusion calculations	✗
	ENEA:	- ERO and plasma modelling for GYM	✓
	FZJ:	- Global material migration in 3D, ERO2.0-EMC3 - 3D modelling for W7-X - Modelling of W dust (-> DEMO) - Numerical studies on surface morphology - CRDS (isotope exchange, retention/release)	✓ ✓ ✓ ✓ ✓
	IPP:	- WallDYN for W7-X	✓
	KIT:	- Neutrals modelling in W7-X divertor	✓

Summary (cont´d)

SubProject	Tasks in 2020		Status
SP4.2 ff	ÖAW:	- MD and potential energy development - Electron impact cross sections	✓ (✓)
	VTT:	- Migration of 2019 AUG experiments - Migration, erosion, deposition for JET-ILW - MD modelling: morphology - Fuel recycling (for ELMs)	✓ ✓ ✓ ✗
SP4.4	CEA:	- SOLEDGE2D-EIRENE for WEST (C4 (He&D)) - 3D turbulence in WEST - SOLEDGE2D–ERO2.0 for W sources and transport in WEST (C4)	✓ ✓ ✓
	IPP.CR:	- PIC simulations with SPICE	✓
	VR:	- Sheath formation modelling	✓

SP4.1 Plasma background and plasma sheath modelling

CEA task

A. Michau et al.

SP4.1 Dust modelling (CEA)

1) Nanoparticle formation along with microparticles under anomalous events : disruptions, VDE, etc.

- Tungsten micro-particles have been readily observed in tokamaks.
- Their production was attributed to anomalous events that yield high energy density deposition at the surface (disruption, VDE, etc.)
- Question addressed: what about the simultaneous production of NP's ?

- High power density disruption (10 MW/cm^2)
- Tungsten melting
- Tungsten vapor emission
- Vapor cooling

→ Nucleation

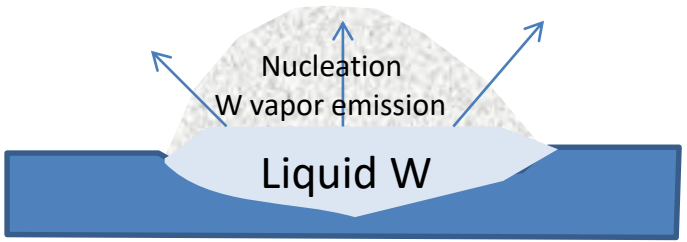

SP4.1 Dust modelling (CEA)

1) Nanoparticle formation along with microparticles under anomalous events : disruptions, VDE, etc.

Methodology:

- Solve for the vapor transport equation under a given non equilibrium state
- Use Classical homogeneous nucleation theory

➔ infer the critical size nucleus and the nucleation kinetics as function of the non-equilibrium state, i.e., the difference between the liquid tungsten and the surrounding low pressure gas

➔ conclude if gas phase nucleation of nanometer size particles is thermodynamically allowed (preliminary)

SP4.1 Dust modelling (CEA)

1) Nanoparticle formation along with microparticles under anomalous events : disruptions, VDE, etc.

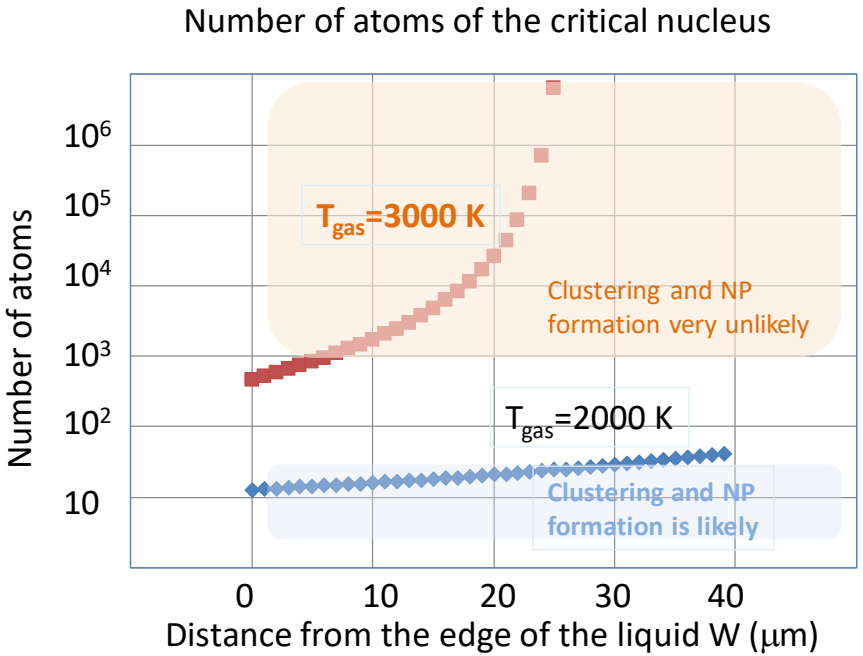

Larger the size of the critical nucleus smaller is the probability of clustering and NPs Formation

➔ Clustering and nucleation are likely for large non equilibrium conditions, i.e. large T_f-T_{gas}

SP4.1 Dust modelling (CEA)

2) Clustering & nanoparticle nucleation under standard plasma conditions

Laboratory experiments show that if neutral density and charged species residence time is high enough and temperature is not too high (this is the case of foreseen detached or semi-detached plasma conditions) **sputtered species may undergo clustering**

- Objective : evaluation of the clustering kinetics

Remark : although W clusters or NPs are just transient species and do not survive in the plasma, they may significantly affect the behavior (radiation, impurity transport, etc.) in the edge plasma.

- **Physics :**

W sputtering or self-sputtering followed by clustering processes with atoms and ions present in near surface plasma :

$W + W \rightarrow W2$; $W + W^{+} \rightarrow W_2^{+}$, ; …; $W + W_n^{m+} \rightarrow W_{n+1}^{m+}$ ….

SP4.1 Dust modelling (CEA)

2) Clustering & nanoparticle nucleation under standard plasma conditions

Starting with cloud of n=6-50 free W atoms randomly located in a 25x25x25 nm^3, follow condensation kinetics as function of temperature during 500 ps. We use EAM potential with Berendsen Thermostat

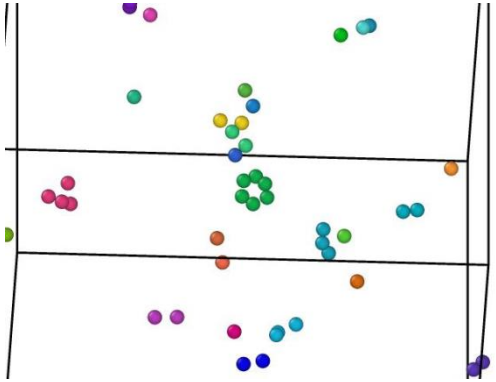

Evidence of clustering with formation of 6-atom cluster

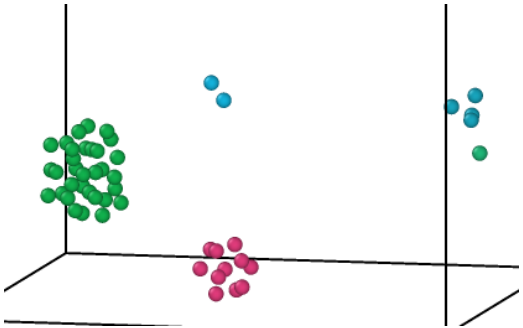

Enhanced molecular growth with formation of up to 50-atom 'amorphous' cluster

Example of large clusters formed in MD simulation N=10-50 & 100

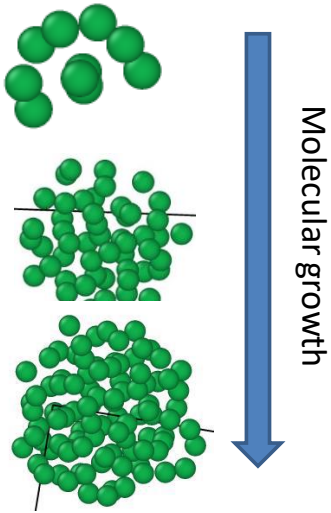

IPP.CR task

D. Tskhakaya et al.

SP4.1 PIC sheath modelling (IPP.CR)

1) 1D Modelling of JET SOL with DT plasma

Ne seeded high recycling SOL plasma for different D/T ratio 25/75, 50/50, 75/25

(CPU time ~ 3 M hours, collaboration with WP-JET1)

- In all cases the D/T density ratio stay almost constant along the flux tube except the divertor plasma, where it increases 10 – 60%.
- All plasma parameters, PWI and kinetic factors are similar to pure D (or T) plasma.
- Next task: perform ELM simulations (as soon as ELM parameters will be provided).

2) Modelling of diffusive sheath

Set of plasma sheath modelling has been performed to study new properties of the diffusive sheath *(CPU time ~5 M hours, collaboration with TSVV task EBC)*

- For high density ($n > 10^{21}$ m^{-3}) divertor plasma ion parallel flux stay subsonic (as predicted earlier *[Tskhakaya PSI 2018]).* Therefore, the actual values of the divertor particle and heat loads are by the factor 2 and more lower than ones obtained from classical sheath model. Corresponding paper under preparation.
- The both, ion-electron as well as ion-neutral frictions contribute to this effect (see figure on next slide)

2) Modelling of diffusive sheath

Poloidal profiles of the parallel Mach number for different divertor plasmas.

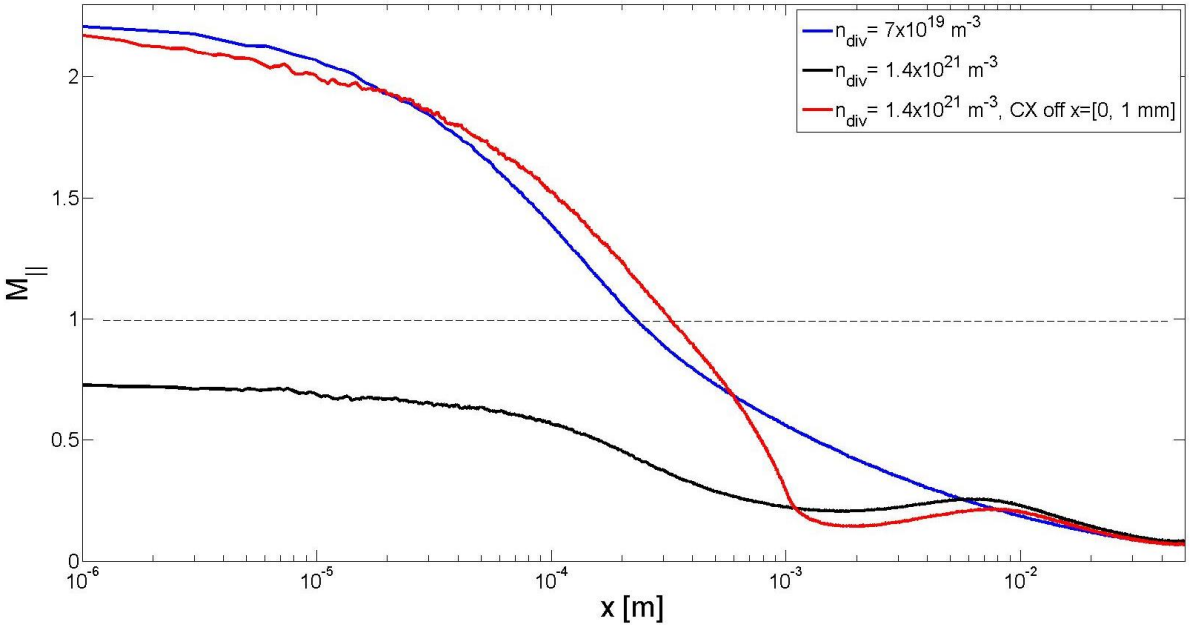

B= 3T, inclination of B field 5°, $T_e = T_i$ ~ 1-2 eV.

Simulations include el, D^+ ions and D neutrals recycled from the divertor plates (located at x=0).

SP4.1 PIC sheath modelling (IPP.CR)

3) Implementation of neutral-neutral collisions in BIT1/BIT3

- Neutral-neutral particle collisions can not be neglected in high density divertor plasma. Accordingly, new collision operators have been developed and implemented in BIT1 and BIT3 codes.
- Test simulations indicate that for high density divertor modelling neutral particle isotropic scattering model is not appropriate and realistic collision models incorporating differential cross-sections are required.

Other tasks relevant to WP-PFC

1. Large set of BIT1 simulations of the COMPASS SOL has been completed. 1 published (2020), 3 accepted, 1 submitted papers. Simulation results agree well with the experiment
2. Kinetic modelling of the COMPASS-U tokamak and ITER SOLs is ongoing

VTT task

M. Groth et al.

SP4.1 Plasma background modelling (VTT)

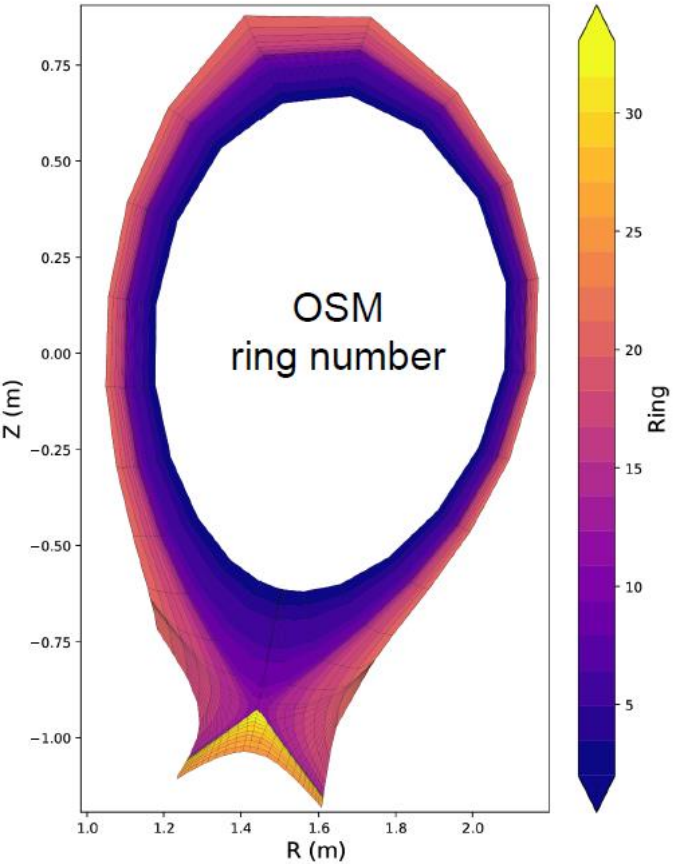

OSM/EIRENE 2007 was debugged and successfully run on grid produced by SOLPS-ITER (Uccello, Sala, Poli. Torino, Lisgo)

Re-establish OSM/EIRENE as a background plasma solver for material erosion and migration tool:

- *Primary application to low-recycling conditions*
- *Assessment and isolation of physics models assessment, data consistency*

First OSM/EIRENE 2007 accomplished

⇒ *systematic scans in divertor target conditions*

⇒ ***input to ERO W erosion simulations (AUG, L-Mode) -> SP4.2***

E. Ihalainen, V. Solokha, H. Kumpulainen

SP4.1 Plasma background modelling (VTT)

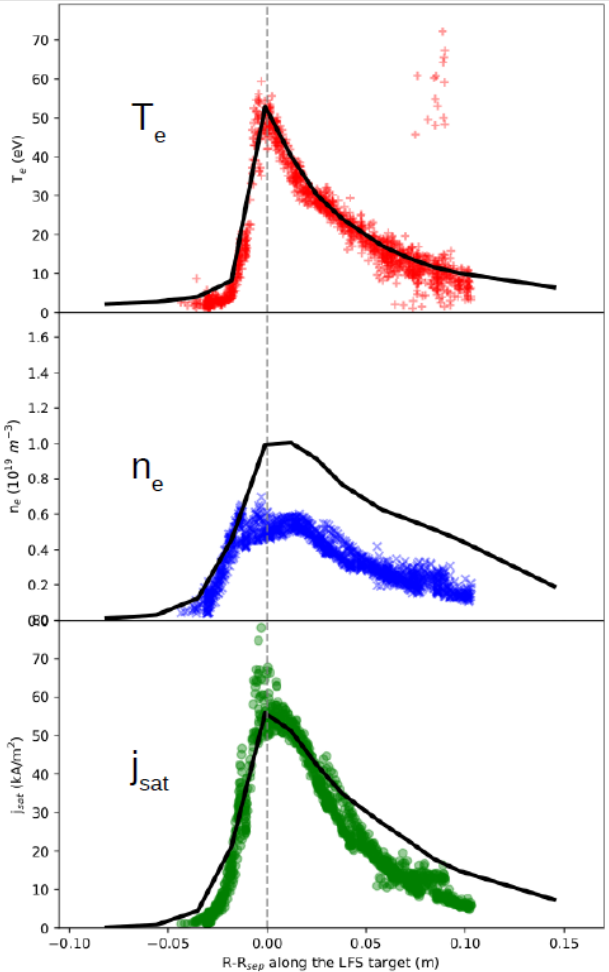

- EDGE2D-EIRENE background L-Mode plasma of JET-ILW, fitted to upstream and target measurements
- Used as input for ERO2.0 (SP4.2)

SP4.2 Plasma-surface interaction and transport modelling

CEA task

Y. Ferro et al.

SP4.2 DFT, diffusion calculations (CEA)

Postponed to 2021

ENEA task

M. Passoni, M. Sala, A. Ucello, E. Vassallo, et al.

SP4.2 ERO and plasma modelling for GYM (ENEA)

- Modelling plasma transport in GyM using the SOLPS-ITER code: simulation of different plasma species (deuterium, helium, argon..) and conditions
- Modelling the surface evolution in plasma-material interaction using ERO2.0

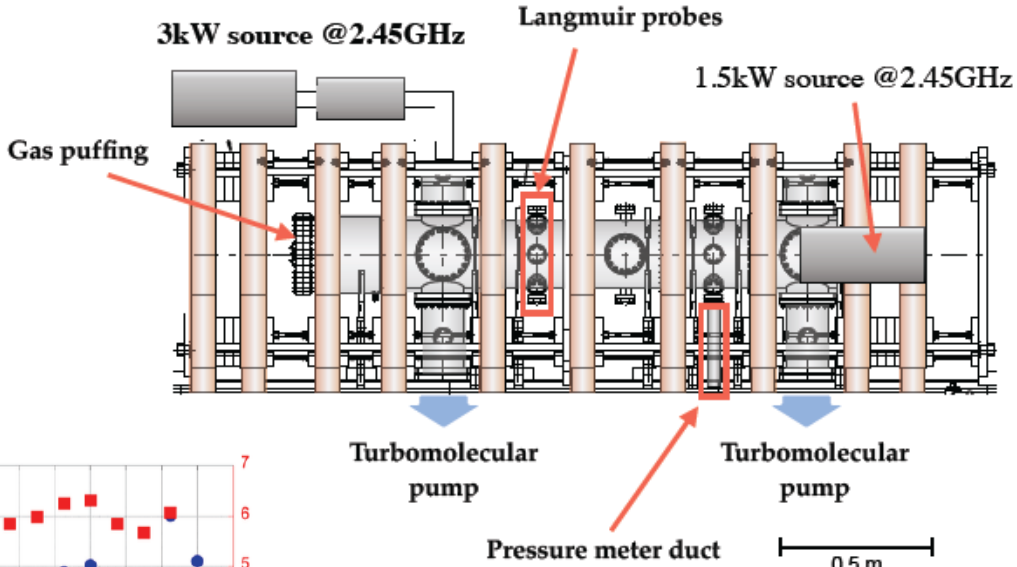

SP4.2 ERO and plasma modelling for GYM (ENEA)

1) Plasma modelling

i) Simulation of Ar plasma in GyM LPD, using SOLPS-ITER

- Geometry transformation from toroidal to linear, definition of code equations for LPDs.
- Comparison with experimental data.

ii) Simulation of He plasma in GyM LPD and development of 0D global model for the interpretation of SOLPS-ITER results

iii) Preliminary **simulations with SOLPS-ITER of the 15kW gyrotron source upgrade** for LPD GyM

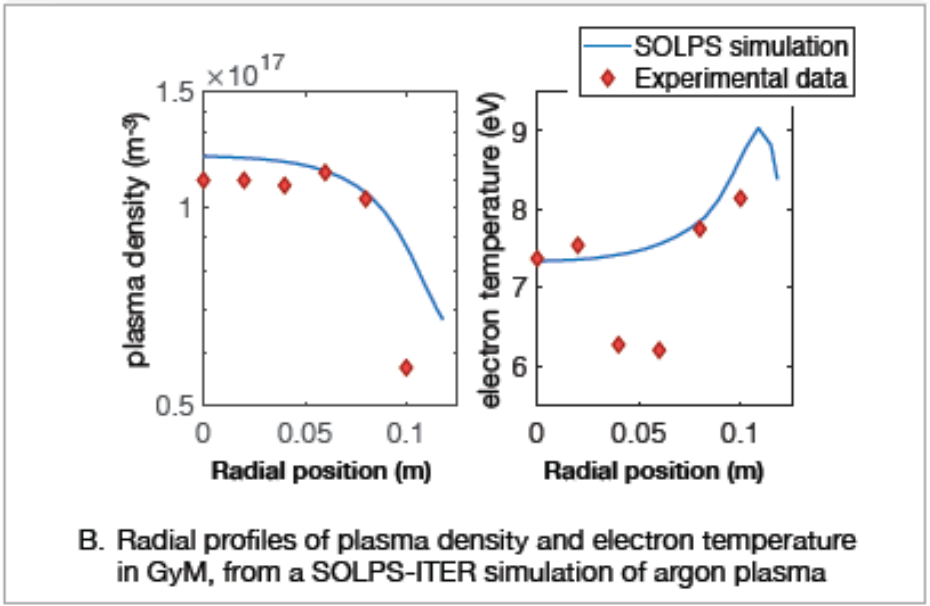

B. Radial profiles of plasma density and electron temperature in GyM, from a SOLPS-ITER simulation of argon plasma

SP4.2 ERO and plasma modelling for GYM (ENEA)

2) ERO2.0 modelling

1. **Comparison between ERO2.0 and a literature model**
   (Skeren et al, New Journ. of Physics, 2013)

Non fusionistic Skeren model solves a differential eq. for surface evolution, accounting for (differently from ERO):

- sputtering dependence on grains orientation
- surface smoothing (diffusion)

Comparison performed on sawtooth W morphology irradiated with 300 eV Ar^+ ions and Single Crystal

Good agreement!

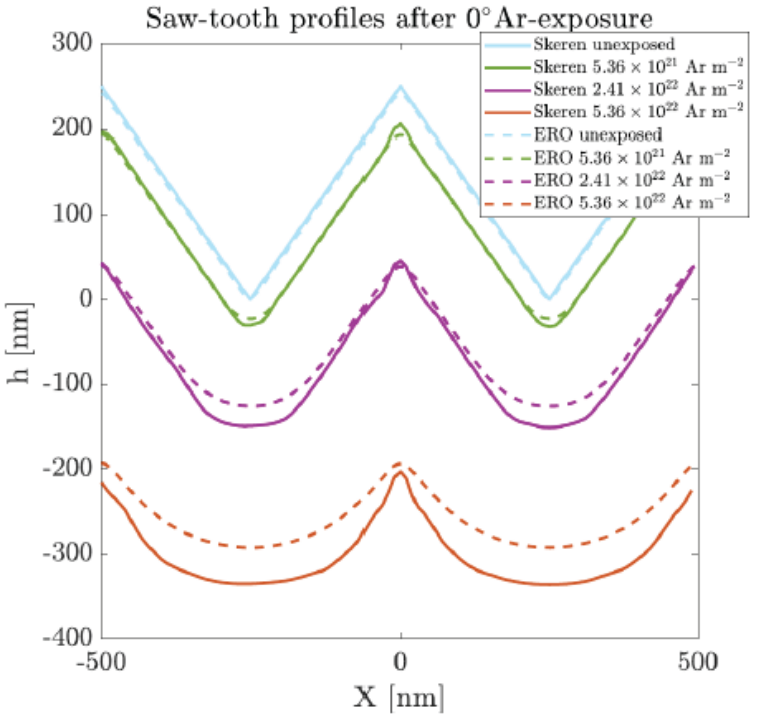

2) ERO2.0 modelling

2. Comparison between ERO2.0 simulations and He-plasma experiments in GyM

- Exposure of W film prepared under SP5.4 to He-plasma in the GyM linear device
- Simulation of the erosion rate performed with and without Sheath Tracing (ST), starting from AFM image of the sample
- Comparison between experimental morphology evolution and ER02.0 simulations with realistic c-W morphology

Open issues...

Related publication: ***Article in preparation***

Good agreement with the ST simulated one!

ERO2.0 w/o ST [at/s]	ERO2.0 with ST [at/s]	Exp. [at/s]
1.02×10^{14}	**2.29×10^{13}**	**1.72×10^{13}**

FZJ tasks

A. Eksaeva, D. Matveev, D. Reiser, J. Romazanov, et al.

SP4.2 CRDS: isotope exchange, retention/release (FZJ)

Example on simulations of baking and cleaning scenarios:

CRDS modelling for JET-ILW M18-30 (Wall cleaning of residual fuel)

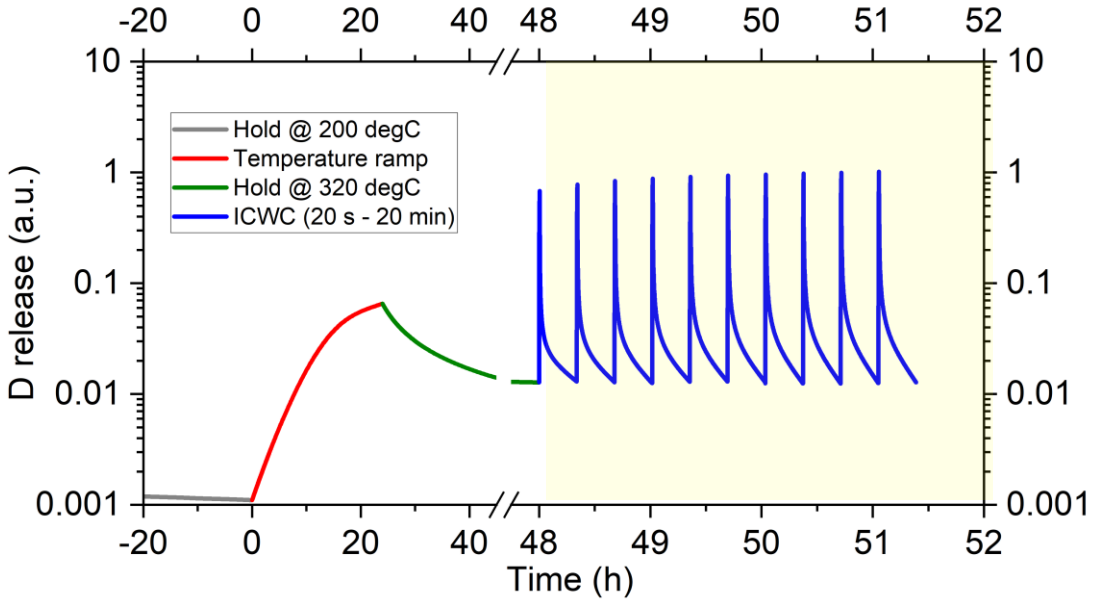

20 μm thick Be layer with 10% D
3 simple trap types: 0.8, 1.1, 1.5 eV

Simulated phases:

- Outgassing prior baking (@200°C)
- Temperature ramp 5 K/h
- 24 h baking @320°C
- 10 ICWC cycles

For global simulation one needs to know retention parameters at various locations depending on layer properties

Motivates studies of co-deposits at JET and laboratory produced Be:D layers

Modelling of TDS data on ILW samples

Here slow decay of outgassing flux during baking of ILW-3 sample is reproduced due to presence of empty traps with weak binding

Trap (i)	1	2	3
E_{dt} [eV]	0.75	1.12	1.35
N_i/N_{total}	30%	15%	55%
Occupancy	2.5%	90%	100%
N_i/N_{total}	25%	30%	45%
Occupancy	1%	60%	90%

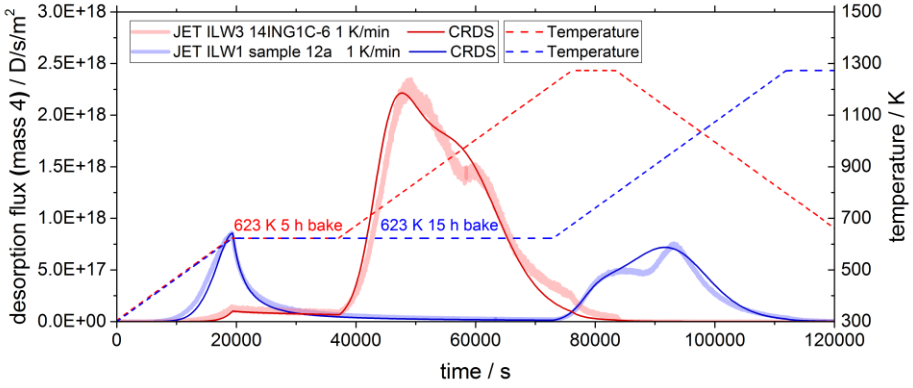

- Model for global fuel removal has to stick to some set of parameters, which are still to be chosen
- Only low accuracy in fitting the data is feasible (no details)
- Further systematic overview of TDS data for other tiles in all campaigns can be helpful to better picture the global dependencies, e.g. more samples from same locations to allow comparable heating rates and baking times

SP4.2 ERO2.0 modelling for “full W ITER” (FZJ)

Motivation: first step to DEMO simulations

List of conducted sensitivity scans:

- Ar, Kr, Ne, Xe impurities (pure D plasma, 0.05%, 0.1%, 0.2%, 0.5%, 1.0%)
- Same tests with an alternative magnetic field configuration (D_{sep} = 4 cm instead of D_{sep} = 9 cm) + with different plasma decay to the wall

Difference to the Be wall:

- No sputtering by D ions, gross erosion is dominated by impurity and W self-sputtering
- 2-25% of W migrates from the wall to the divertor
- **With impurities:** all values (deposition, gross/net erosion, W self-sputtering) are increased by a factor 10^1-10^2

SP4.2 ERO2.0 modelling for “full W ITER” (FZJ)

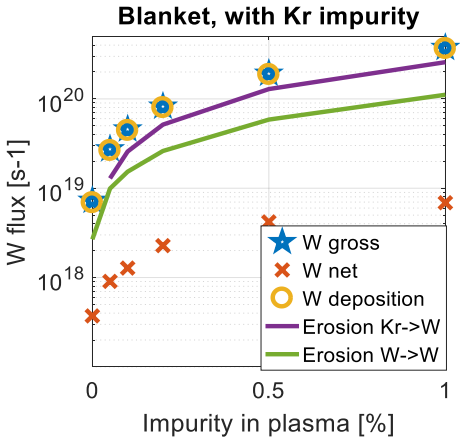

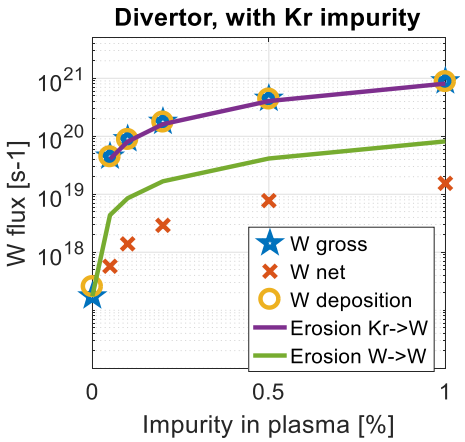

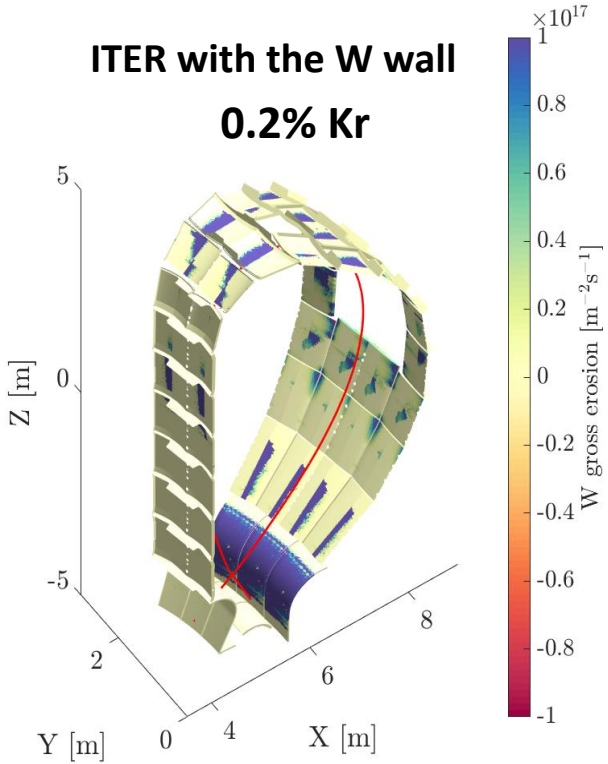

Post processing:

- Dust formation (deposits, conversion factor 100%)
- Tritium retention (co-deposition, scaling of G. De Temmerman)

Uncertainties:

- No feedback from impurities to the plasma
- Dust conversion factor
- Surface roughness effect

SP4.2 ERO2.0 modelling of W7-X experiments (FZJ)

- Carbon molecular processes were implemented (CH_4 ionisation-dissociation chain)
- EMC3-EIRENE plasma backgrounds and 3D wall geometry were imported

- **Simulations of global ^{12}C erosion and transport:**
- 36° toroidal sector modelled, assuming periodic boundaries
- Considered erosion processes: Erosion of ^{12}C by H impact (phys. & chem. erosion) and C self-sputtering
- Synthetic spectroscopy signals (CI, CII, CIII) produced for different QSS diagnostics → comparison with experiments ongoing
- C net erosion poloidal profiles along divertor marker fingers produced → comparison with post-mortem results ongoing; Mo erosion and transport to be included in future simulations

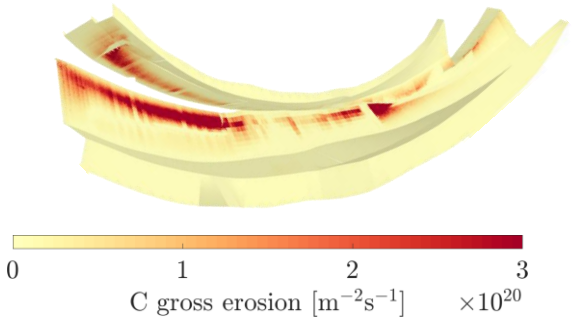

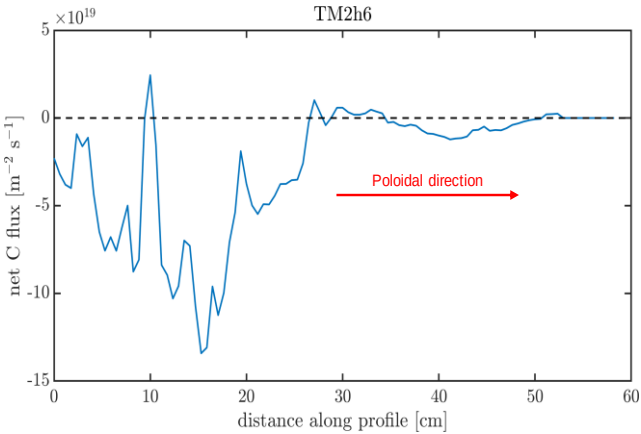

SP4.2 ERO2.0 modelling of W7-X experiments (FZJ)

- **Simulations of ^{13}C injection and global transport:**
  - simulation domain was extended to full 360° simulation without periodic boundaries
  - injection of 1e20 $^{13}CH_4$/s from nozzle at divertor target in module M3 bottom part
  - transport, reflection and deposition of ^{13}C was tracked in the torus → high local deposition in M3 bottom but also deposition found in other modules, especially M1
  - re-erosion of ^{13}C not considered yet → to be included in follow-up simulations (mixing model and multi-step runs required, much more computationally demanding than the initial first-flight simulations)

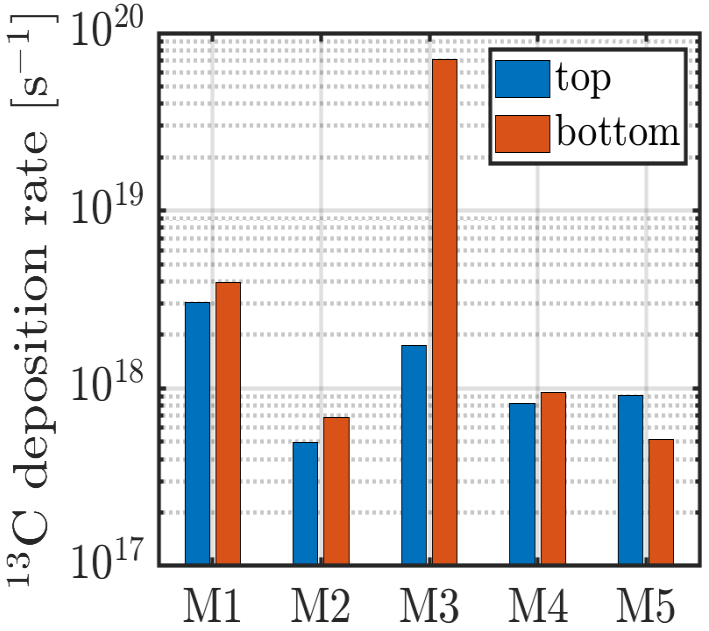

- **Remark: application to ITER with RMPs upcoming**

SP4.2 Numerical studies on surface morphology (FZJ)

Determine macroscopic parameters in Kuramoto-Sivashinsky-Model by the use of experimental data to obtain a physics driven model.

- The numerical toolbox has been extended by inclusion of Ridge Regression, and LASSO method to the Least-Squares-Analysis approach.
- Additionally a Genetic Algorithm has been developed, coded and extensively tested with data from plasma assisted conversion of hydrocarbons.
- The ion beam experiments have not been conducted at FZJ, but another collaboration has been initiated with HZDR.
- First data are available since September 2020 and 2D surface data analysis is ongoing.

DATA FOR LINEAR REGRESSION MODEL DISCOVERY

Example of AFM data available since Sep 2020

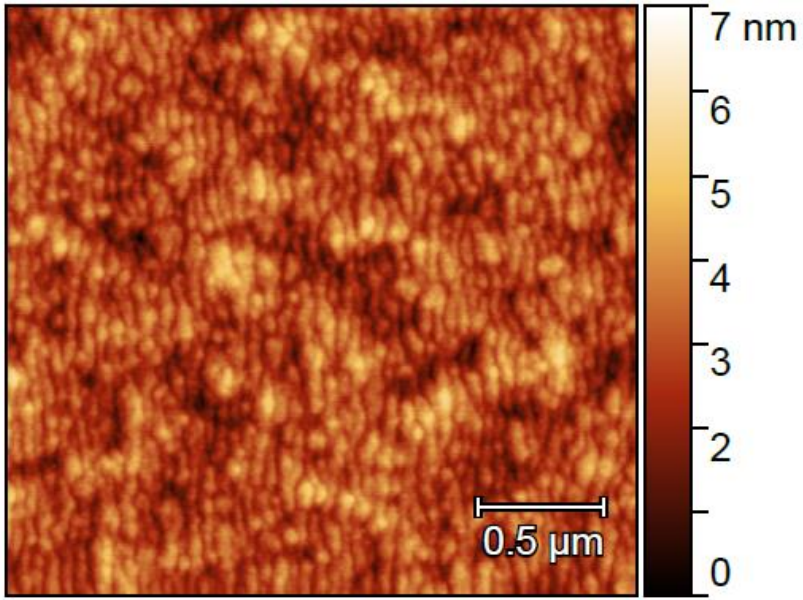

Parts of this research were carried out at the Ion Beam Center of the Helmholtz-Zentrum Dresden-Rossendorf.

We would like to thank Dr. D.J. Erb and Dr. S. Facsko for assistance.

IPP task

K. Schmid et al.

SP4.2 WallDYN (3D) for W7-X (IPP)

- **Total ^{13}C deposition after 400 seconds of seeding**
- **Three main deposition regions**
  - **#1 & #2 direct deposition from valve "Bifurcation" in magnetic island**
  - **#3 from re-erosion and multi-step transport**
- **Little deposition on strike line (too high T_e)**

Total ^{13}C deposition

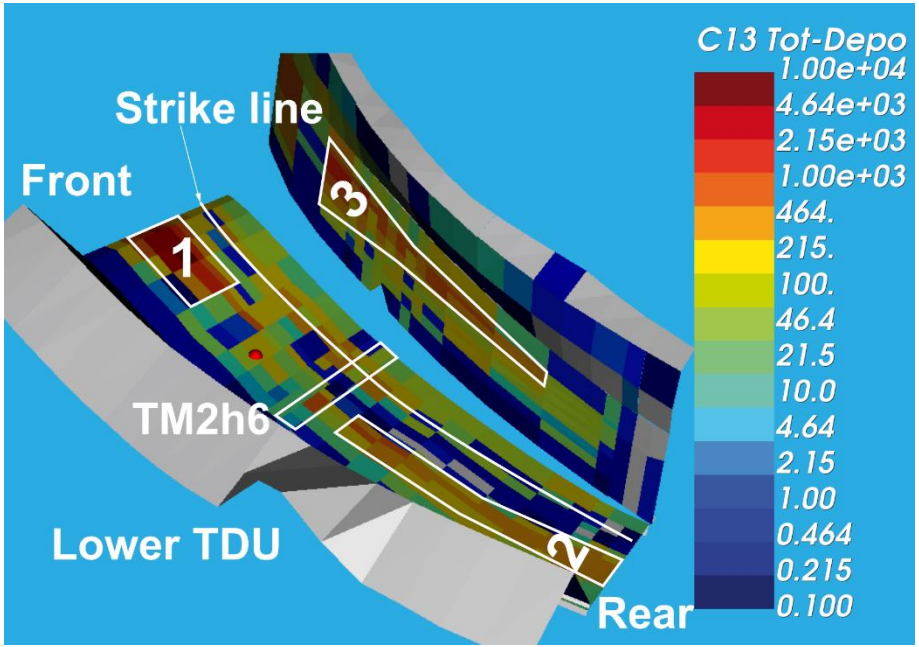

SP4.2 WallDYN (3D) for W7-X (IPP)

- **Compare to first preliminary post mortem analysis of ^{13}C deposition by M. Mayer**

- **WallDYN 100%**
  (no loss to other simulation volumes)
  = Upper boundary

- **WallDYN 50%**
  (50% loss to other simulation volumes)
  = Lower boundary

Comparison to post mortem results

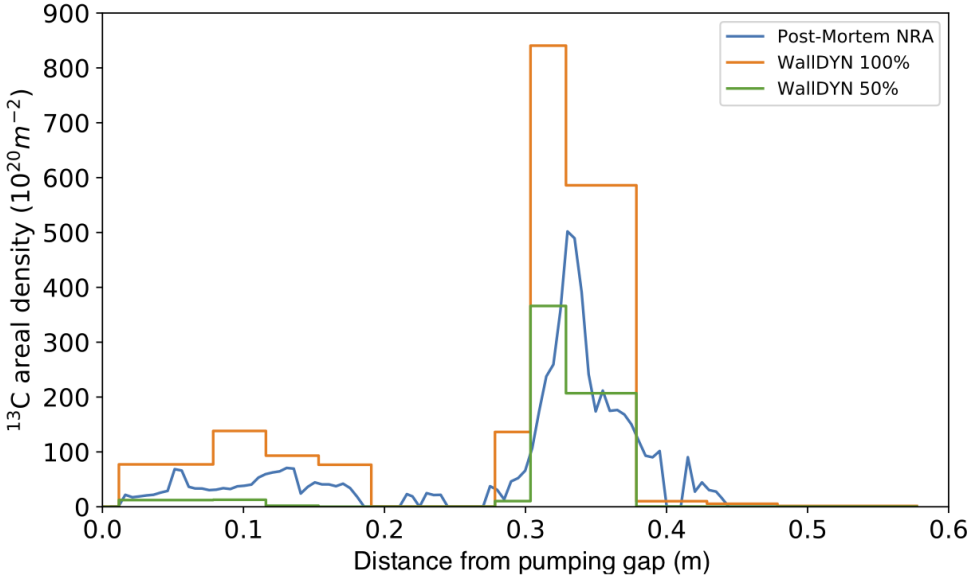

→ **Good qualitative and even quantitative agreement**

SP4.2 WallDYN (3D) for W7-X (IPP)

- **Local balance of influx and loss channels**
  - **Dominated by influx from value**
    - Clear deposition region
  - **Domiated by re-erosion sources and multi-step migration.**
    - Delicate balance
      Influx wins by small margin

Requires integrated modeling of surface & plasma transport

Erosion deposition balance

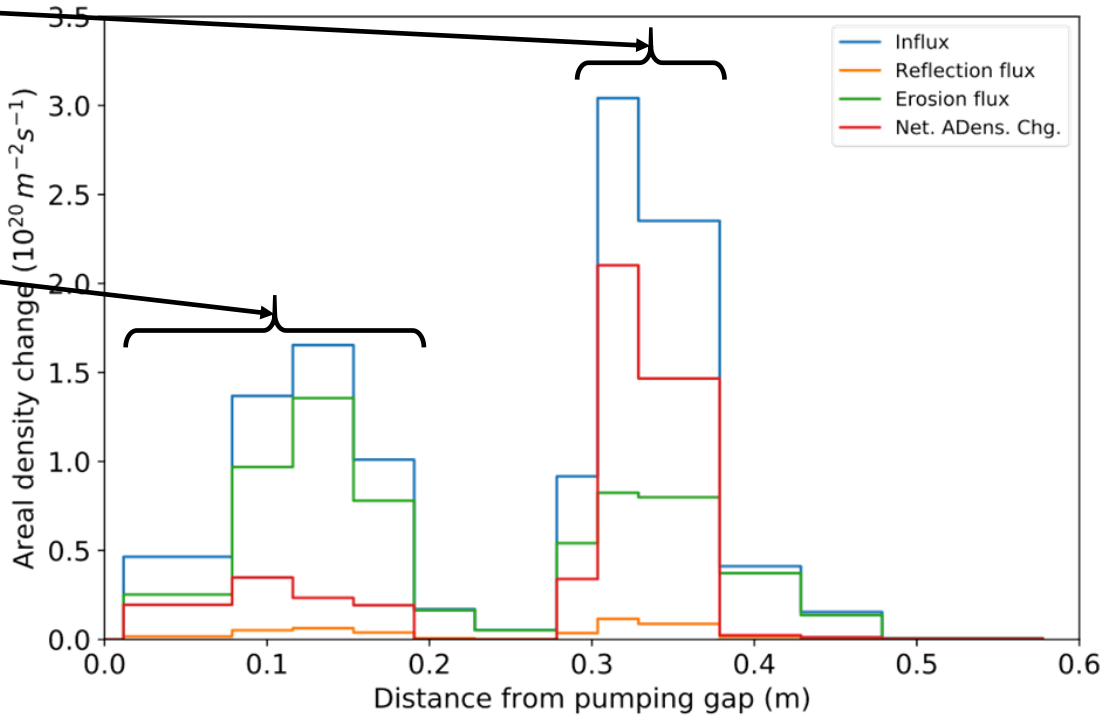

SP4.2 WallDYN (3D) for W7-X (IPP)

^{13}C sources

❖ Local ^{13}C influx is due to different sources: Seeding, re-erosion and reflection

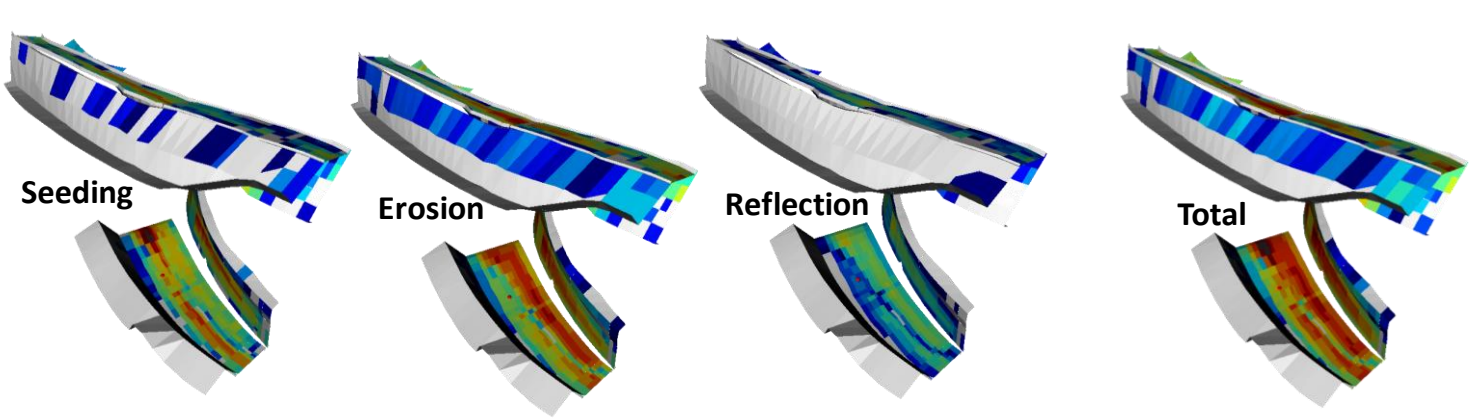

- Erosion and seeding dominate influx
- Influx at strike line dominated by re-erosion sources
- Reflection only has minor impact (low R-yield for C on C would be different for Be on W)

Requires integrated modeling of surface & plasma transport

KIT task

S. Varoutis, C. Tantos, Yu. Igitkhanov, Ch. Day

SP4.2 Neutrals modelling in W7-X divertor (KIT)

- Assessement on influence of various geometrical and flow parameters of W7X particle exhaust system. Numerical analysis focused on operation phase OP1.2b.
- Numerical code DIVGAS (particle-based method, solution of Boltzmann equation).

- Studying implication of gaps, slits and other leakages at different positions at the targets and the poloidal closures.
- Influence of pumping gap panel on divertor pumping efficiency.
- Effect of different surface temperatures on neutral gas flow in sub-divertor region.
- DIVGAS comparison with experimental results (pressure measurements at AEP, AEH positions) for different plasma scenarios (standard and high-iota-configuration) as well as for different pumping scenarios (with/without AEP and with/without AEH), defining simplified input parameters (influx rate through pumping gap).

SP4.2 Neutrals modelling in W7-X divertor (KIT)

Assumptions & results

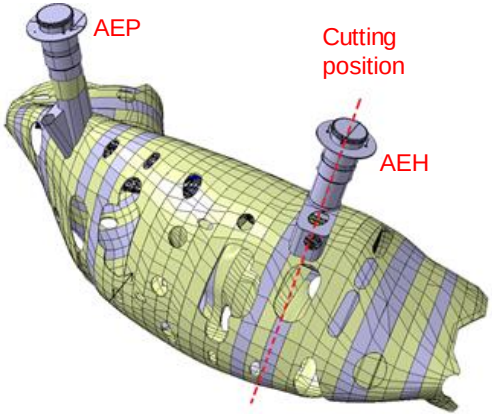

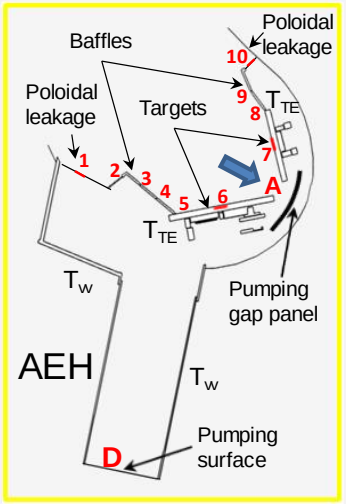

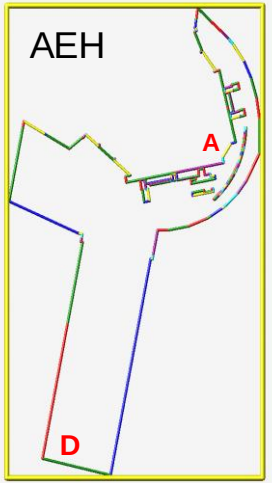

- 2D represented flow fields of AEH and AEP ports extracted from 3D CATIA files.
- Reference influx rate through pumping gap (surface A) has been assumed 10^{20} s^{-1}. Temperature of vacuum vessel is 303 K, temperature at targets is: 400-1000 K.
- Influence of target temperature on flux through gap leakages is rather weak.
- Presence of pumping gap panel: 12% increase of neutral outflux, 25% decrease of pumped flux.

SP4.2 Neutrals modelling in W7-X divertor (KIT)

Results (cont.)

- Increasing influx rate by order of magnitude: increase in outflux (~2%) and in pumped flux (~9%). Corresponding divertor gas collisionality increases by order of magnitude.
- Closure of poloidal leakages facilitates increase of pumped flux by ~20% as well as neutral outflux towards the plasma by ~5%.
- 2D representation of sub-divertor seems to be insufficient for comparing numerical and experimental results. This work is still on going.

Outlook

- Effect of gas impurities such as Ne and N in comparison to experiment (2D sub-divertor configuration)
- 3D DIVGAS runs with realistic plasma background and compare with experimental results
- Implication of gaps, slits, other leakages at different positions at targets and poloidal closures with DIVGAS for the case of a 3D sub-divertor
- 3D DIVGAS simulations considering a cryopump in sub-divertor

ÖAW tasks

M. Probst et al.

SP4.2 MD and potential energy development (ÖAW)

Machine-Learning Potential energy function developments and MD simulations
(work mostly performed by L. Chen and S. Shermukhamedov)

Example:

Be sputtering yield on a $Be_2W(001)$ surface. Non-cumulative D impact with 10 to 100 eV. Dependence on incident angle (0°, 20°, 45° and 60°).
(Comparison with MD sputtering yields from Lasa *et al* : Be_2W, non-cumulative D impacts, 90°)

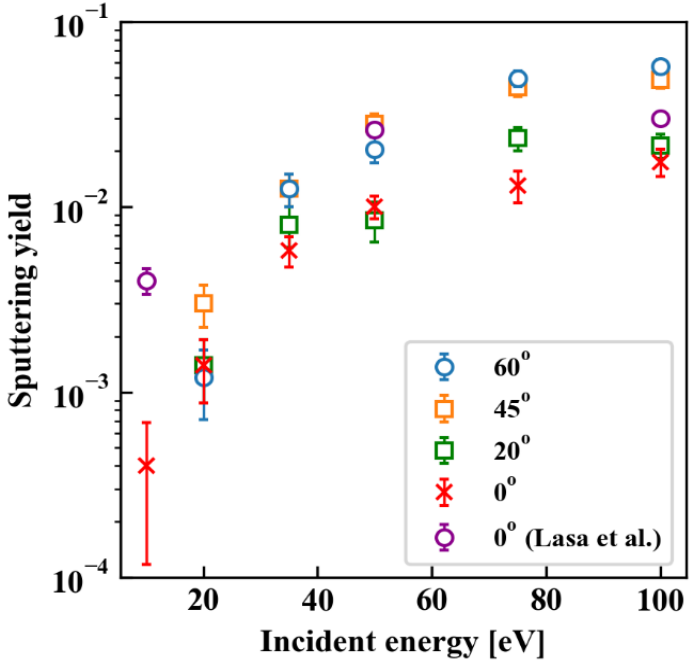

SP4.2 MD and potential energy development (ÖAW)

Machine-Learning Potential energy function developments and MD simulations

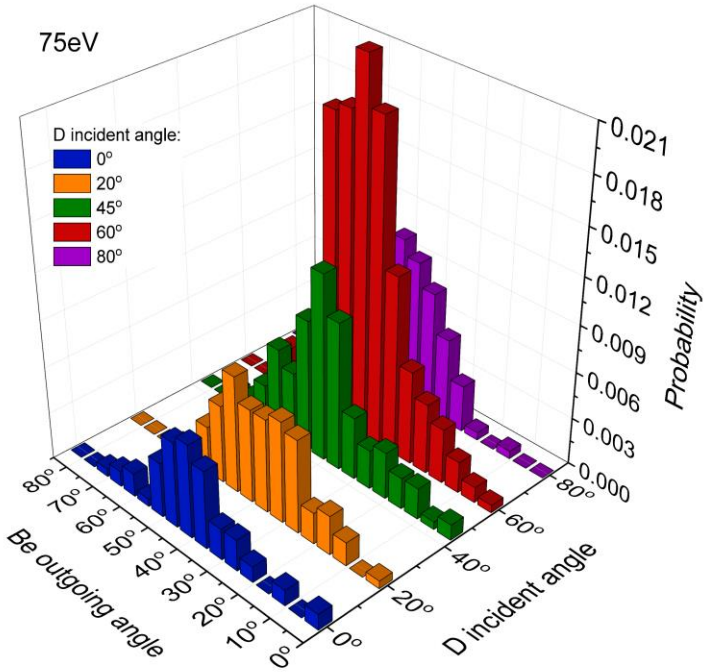

Analysis of angles of the sputtered/reflected particles

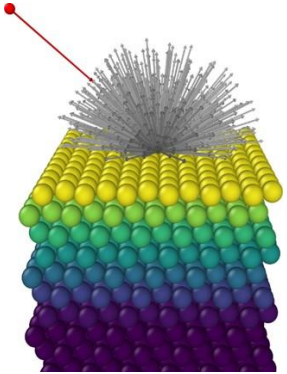

Analysis of the angular distributions of sputtered particles as a function of the angle of impacting D atom.

VTT tasks

A. Hakola, K. Nordlund, F. Granberg, M. Groth, et al.

SP4.2 Nitrogen transport in JET L-Mode plasmas (VTT)

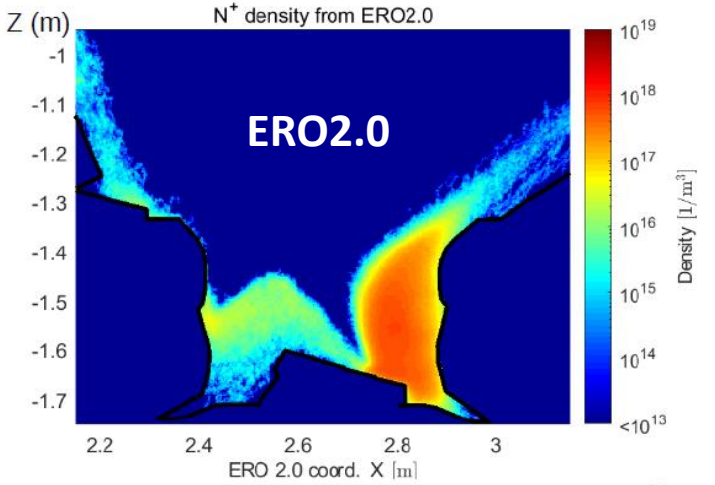

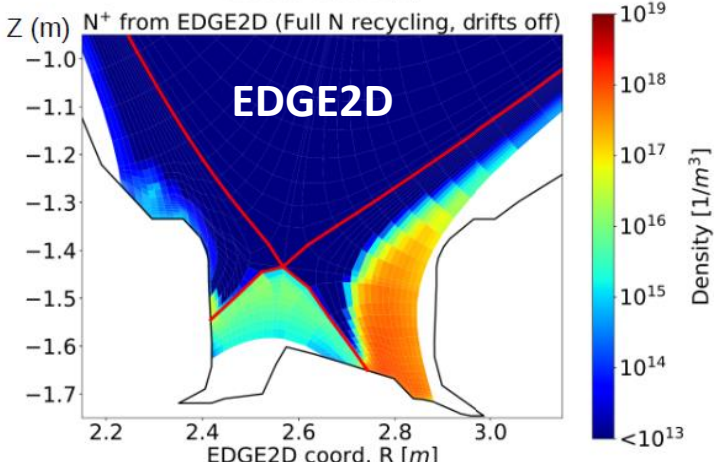

- N_2 and its break-up chain newly implemented and tested in ERO2.0
  - Recycling impurity, removal by pumping
  - EDGE2D-EIRENE background plasma based on a detached L-mode experiment
- Nitrogen density and emission profiles predicted by ERO2.0 and EDGE2D-EIRENE qualitatively similar and same order of magnitude
- With molecular effects included, predicted N II emission is 20% higher than with atomic N injection

Roni Mäenpää

SP4.2 Be erosion & migration in JET-ILW divertor (VTT)

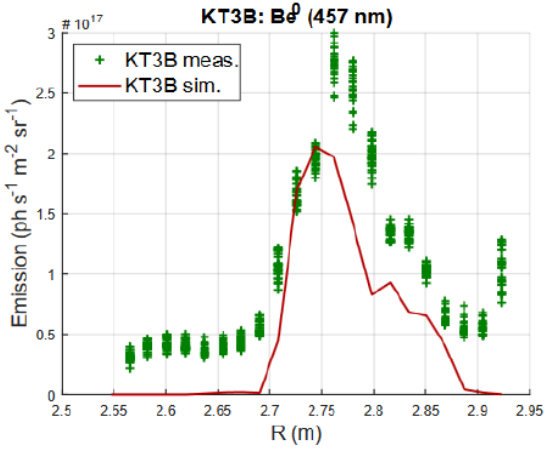

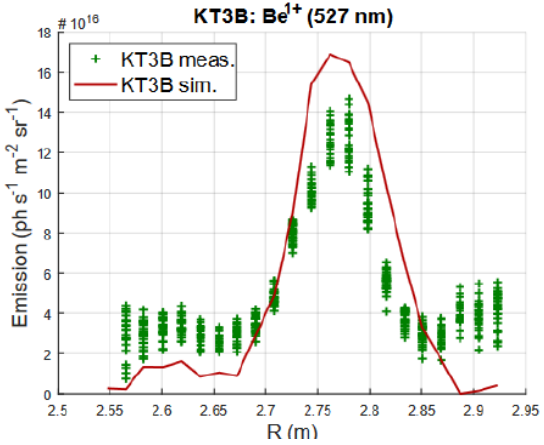

- Interpretative ERO2.0 modelling of a low-recycling L-mode plasma
  - Assumed Be deposits at divertor surfaces were adjusted to match spectroscopy and post-mortem tile analysis
  - Main chamber Be sources included
  - EDGE2D-EIRENE background plasma fitted to upstream and target measurements
- Agreement within 25% reached for simulated and measured Be I and Be II emission at the LFS target
- Be re-erosion from W surfaces identified as the dominant cause of all Be emission lines in the divertor

Henri Brax

SP4.2 Modelling erosion at outer divertor of AUG (VTT)

Starting point: erosion experiment in 2019

- Mo-coated (~200 nm) graphite samples with **1×1 mm² or 5×5 mm² Au marker spots** (thickness ~20 mm) exposed to L-mode plasmas on ASDEX Upgrade (AUG) in 2019
  - ✓ Small marker spots → gross erosion
  - ✓ Bigger marker spots → net erosion
  - ✓ Au (and Mo) proxies for W (AUG is a full W device)
- Main parameters:
  - ✓ B_t = 2.5 T, I_p = 0.8 MA, $n_{e,core}$ ~ 4×10^{19} m^{-3}
  - ✓ P_{ECRH} = 0.8 MW, $T_{e,peak}$ ~20-25 eV, $\tau_{exposure}$ ~ 44 s
- Erosion profiles of the Au markers and the Mo layer measured close to the outer strike point (OSP)

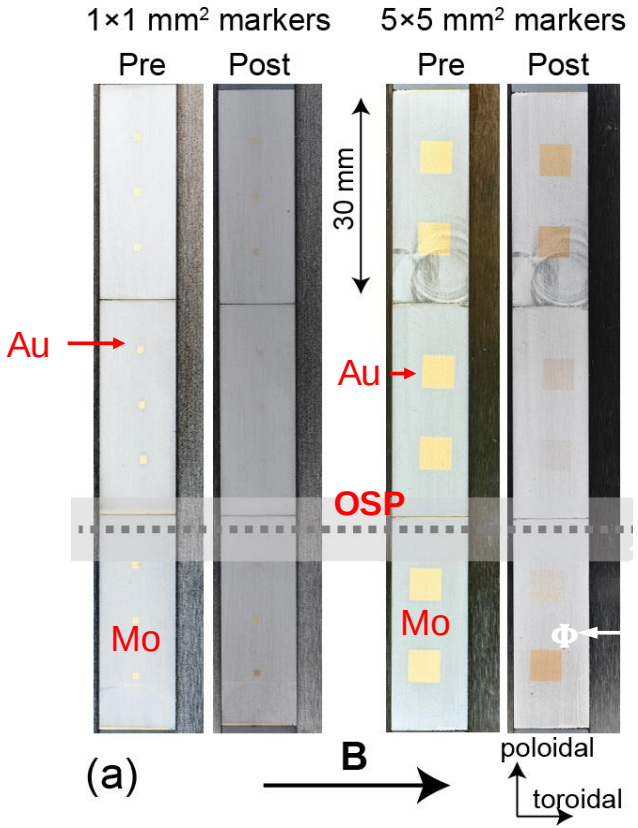

SP4.2 Modelling erosion at outer divertor of AUG (VTT)

- Mo-coated (~200 nm) graphite samples with **1×1 mm² or 5×5 mm² Au marker spots** (thickness ~20 mm) exposed to L-mode plasmas on ASDEX Upgrade (AUG) in 2019
  - ✓ Small marker spots → gross erosion
  - ✓ Bigger marker spots → net erosion
  - ✓ Au (and Mo) proxies for W (AUG is a full W device)
- Main parameters:
  - ✓ B_t = 2.5 T, I_p = 0.8 MA, $n_{e,core}$ ~ 4×10^{19} m^{-3}
  - ✓ P_{ECRH} = 0.8 MW, $T_{e,peak}$ ~20-25 eV, $\tau_{exposure}$ ~ 44 s
- Erosion profiles of the Au markers and the Mo layer measured close to the outer strike point (OSP)

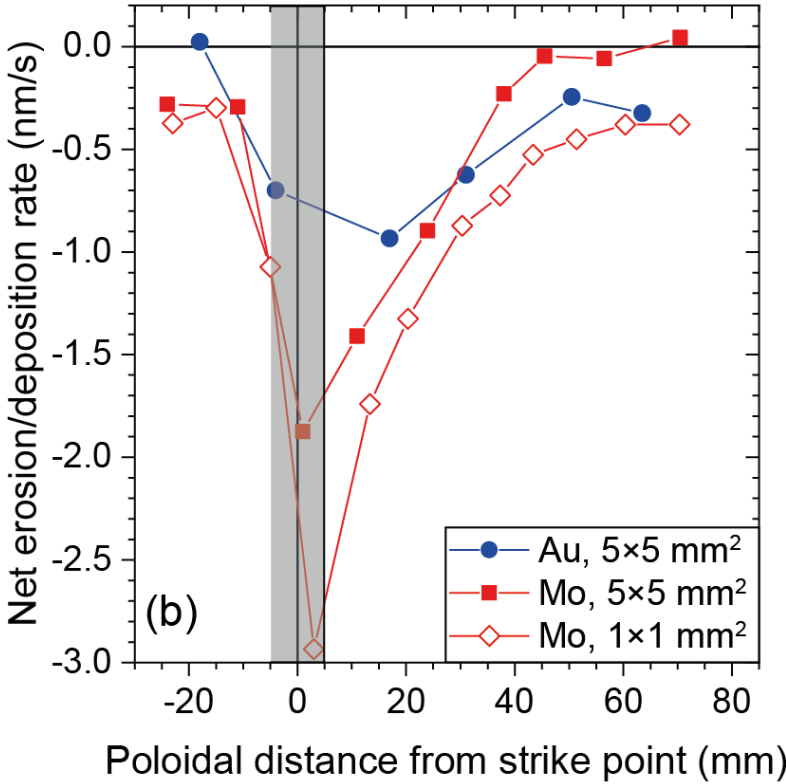

SP4.2 Modelling erosion at outer divertor of AUG (VTT)

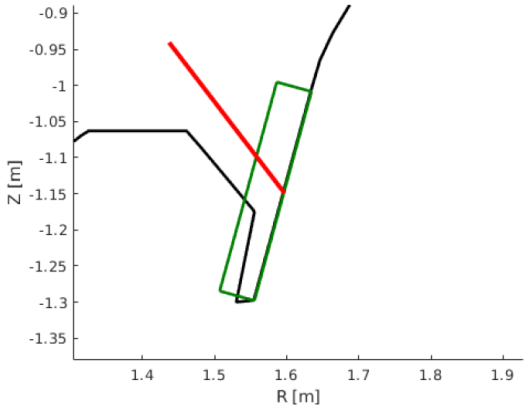

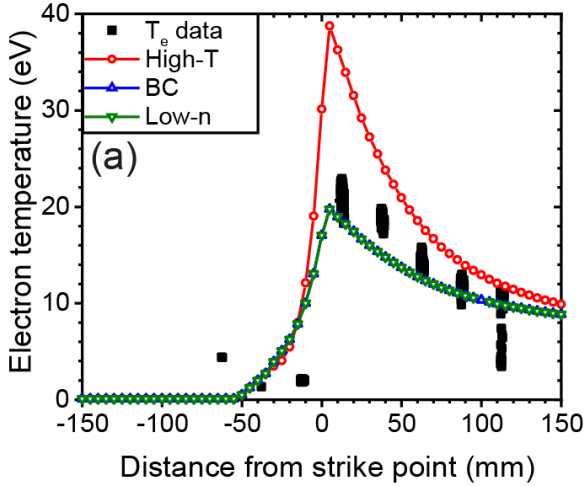

- ERO simulations continued with **corrected OSM plasma backgrounds**
  - ✓ Now possible to investigate the influence of electron density and temperature on erosion/deposition
  - ✓ Impurity concentrations in the plasma varied as before: c_W=0.005-0.01%, c_C, c_N, c_B=0.5-1.0% → relying on typical values in corresponding plasmas (no measurements available)
- Simulated volume selected to **cover the entire "OSP Tile 1"** of the AUG divertor
  - ✓ Dimensions 300×300×50 mm^3

SP4.2 Modelling erosion at outer divertor of AUG (VTT)

ERO results for Au erosion

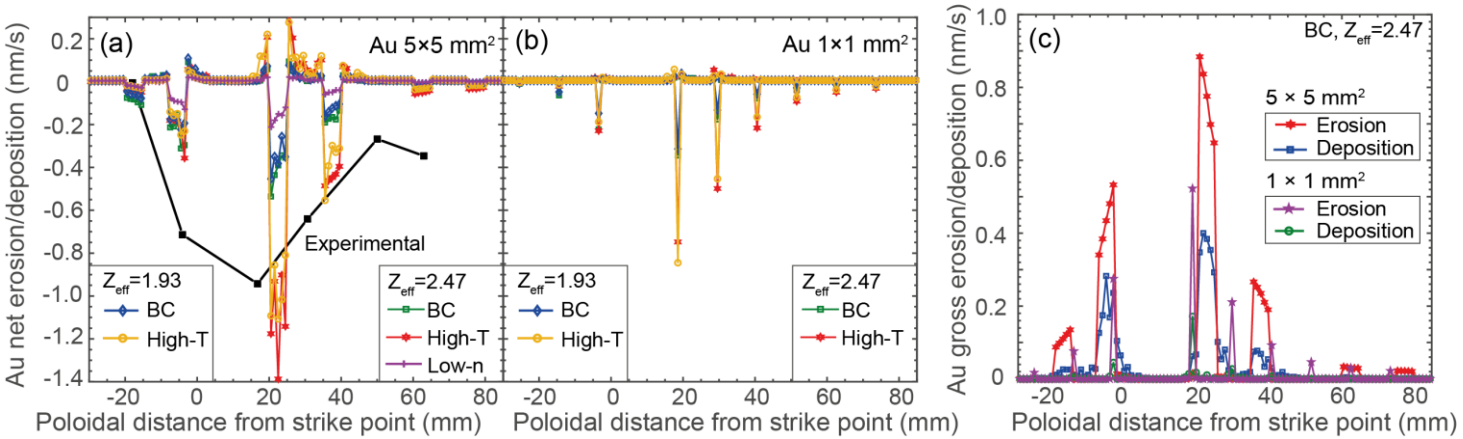

- Simulations with different background plasmas **reproduce the main features** of the experimental net erosion profile of Au
- **T_e has the strongest impact** on erosion: doubling T_e enhances erosion by a factor of 2.5-3
- Discrepancies may be attributed to applied models for T_i, plasma potential, and sheath characteristics in ERO or the applied OSM solutions → to be improved
- No big differences between the different marker sizes except for the vicinity of the strike point region: here **large markers exhibit stronger erosion**!?

SP4.2 Modelling erosion at outer divertor of AUG (VTT)

ERO results for Mo erosion

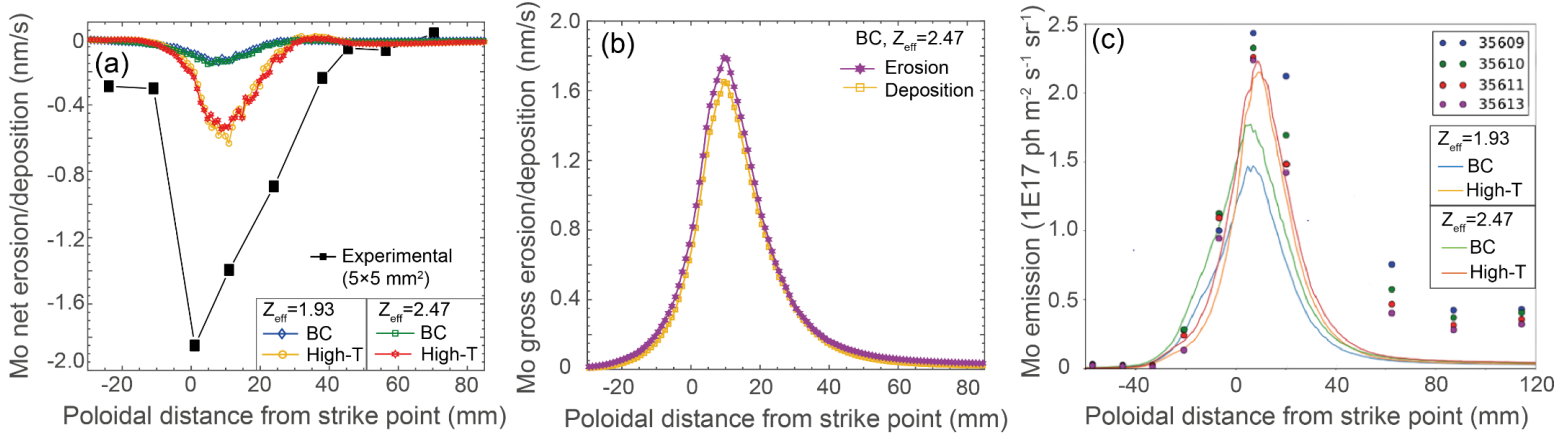

- **Simulated net erosion 3-5 times smaller** than the experimental one, due to
  - ✓ Previously mentioned limitations in the models?
  - ✓ Surrounding areas of the marker samples being covered with impurities and W from previous experiments? → actual re-deposition of Mo reduced?
- **Light impurities (C, N, B) do not have a noticeable effect** on Mo erosion
- Very strong re-deposition predicted while gross erosion agrees with the simple charge-mass estimate (comparison between Au and Mo)

SP4.2 Modelling erosion at outer divertor of AUG (VTT)

Comparison between W and Au

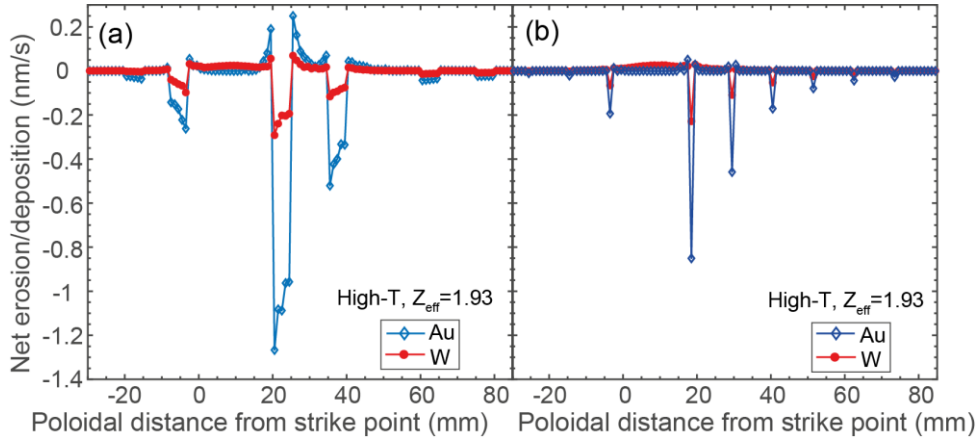

- Au eroded **3-5 times faster** than W
- Largest differences in the strike-point region

- Both Au and W exhibit a **toroidal tail of deposits**
- Majority of the deposition **within 10 mm from the origin**
- Deposition outside the marker spots 2-3 orders of magnitude lower → below detection threshold?

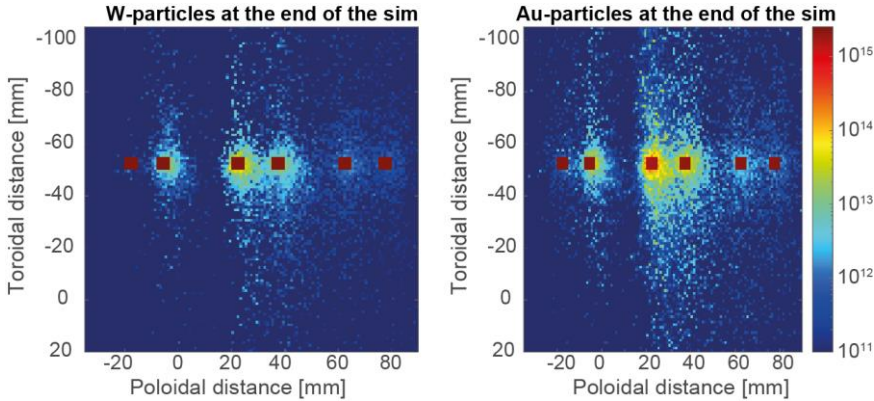

Background

- We have observed that pillars will decrease the sputtering yield
  - Decrease related to the height of the pillar
  - Only atoms on the top of the pillar will sputter easily, for higher heights

Initial structure

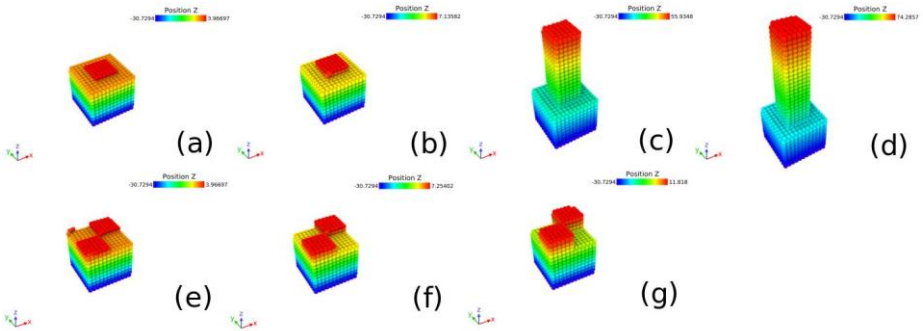

Sputtering frequency

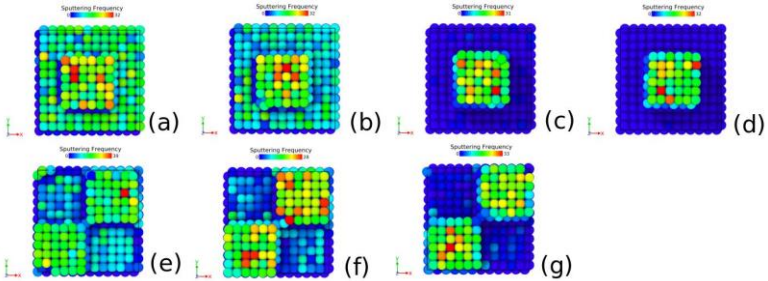

Rough surfaces

- Three setups:
  - Hills of different height
  - Fuzz like structure
  - Foam

Hills

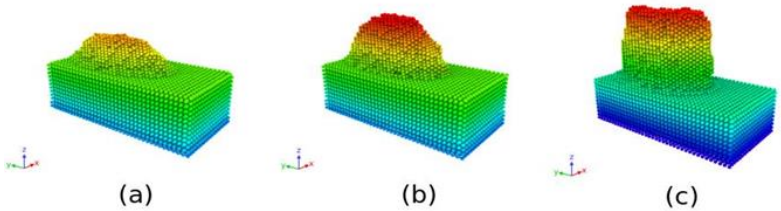

Fuzz like structure

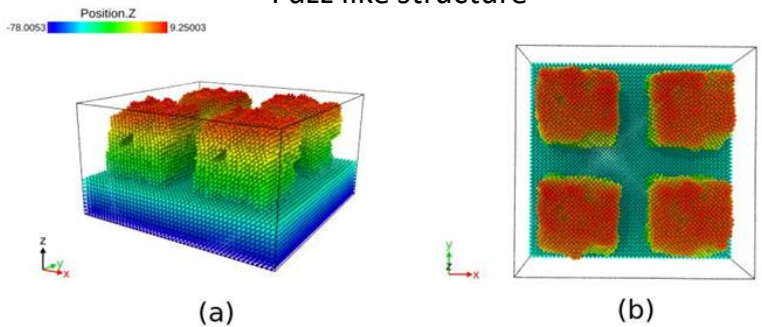

Foam

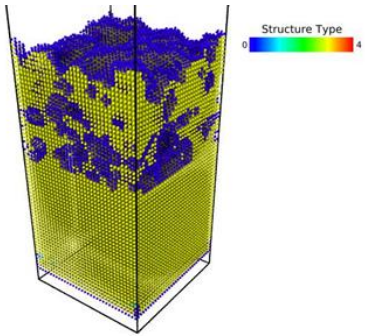

Results and conclusions

- Different angle yields the maximum sputtering (45 vs 60 degrees)
- Fuzz has higher sputtering yield, even though the energy is less
- The higher the hill, the lower the sputtering yield
- The foam has a lower sputtering yield than the perfect surface

Hills 5 keV

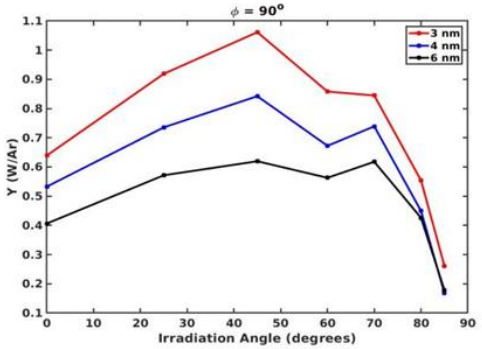

(a)

Fuzz 1 and 2 keV

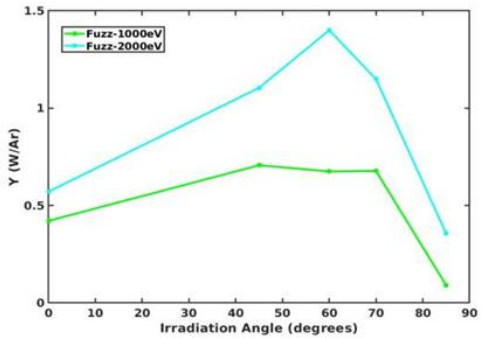

(b)

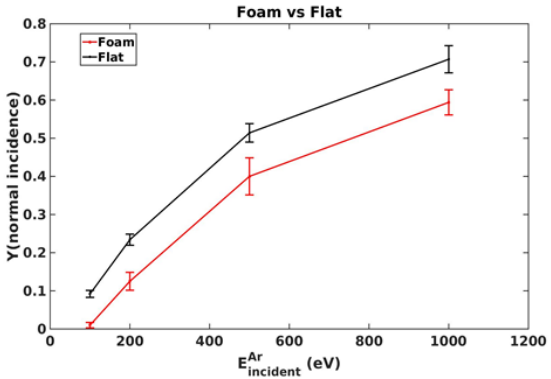

SP4.4 Plasma background and plasma-wall interaction modelling for WEST

CEA tasks

G. Ciraolo, Y. Marandet, et al.

SP4.4 SOLEDGE3X modelling for WEST (CEA)

SOLEDGE3X : fusion of SOLEDGE2D [transport] and TOKAM3X [turbulence] codes

- Solves drift-fluid equations in 2D or 3D (mass, parallel momentum, energy and current balance)
- Based on Zhdanov closure for multi-component plasma : Able to solve arbitrary number of species without trace impurity assumption
- Able to treat complex wall geometry and magnetic configurations
- Includes several neutral models
  - Crude fluid model
  - Kinetic neutrals (EIRENE)
- Quite recent code (Verification and validation ongoing)

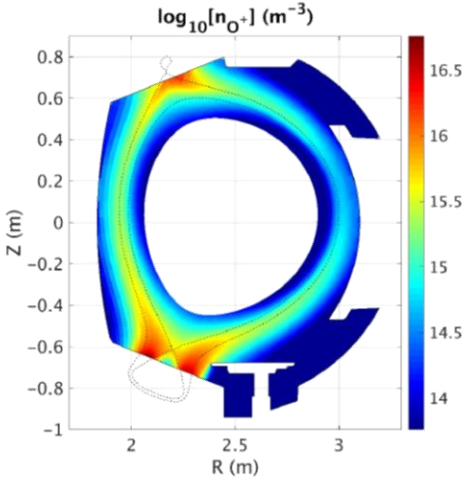

Transport simulation example: Density of Oxygen [O^+] ion

SP4.4 SOLEDGE3X modelling for WEST (CEA)

SOLEDGE3X implements “state of the art” collisional closure for a proper description of multi-component plasmas

- Modelling should help understanding plasma radiation level and pattern
- Application to Oxygen transport in the SOL [**A. Gallo et al., Nuclear Fusion, accepted**]

Exp.: WEST #54067 : $P_{SOL} = 2MW$ ($4MW$ LH heating - $2MW$ bulk radiation)
$n_{lid} = 4 \cdot 10^{19} m^{-2}$ (interferometry)

Simu.: D+O plasma (assumption 2% Oxygen in the core)
ad-hoc perpendicular diffusivity: $D = \nu = \frac{\chi}{2} = 1 m^2 s^{-1}$

SP4.4 SOLEDGE3X modelling for WEST (CEA)

SOLEDGE3X implements “state of the art” collisional closure for a proper description of multi-component plasmas

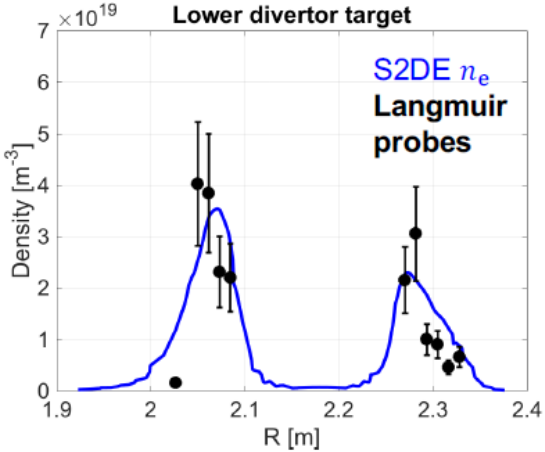

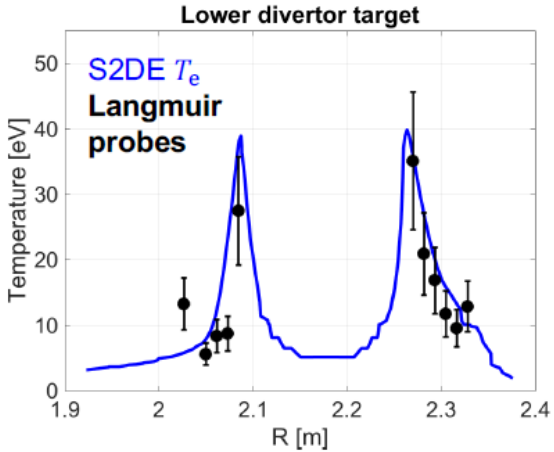

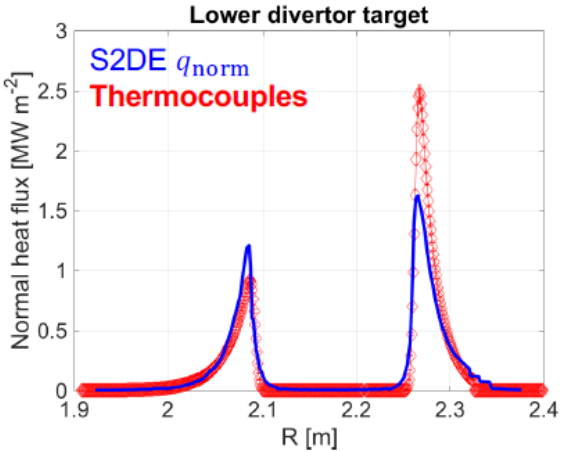

Target profiles (Exp vs Simu).

SP4.4 SOLEDGE3X modelling for WEST (CEA)

SOLEDGE3X implements “state of the art” collisional closure for a proper description of multi-component plasmas

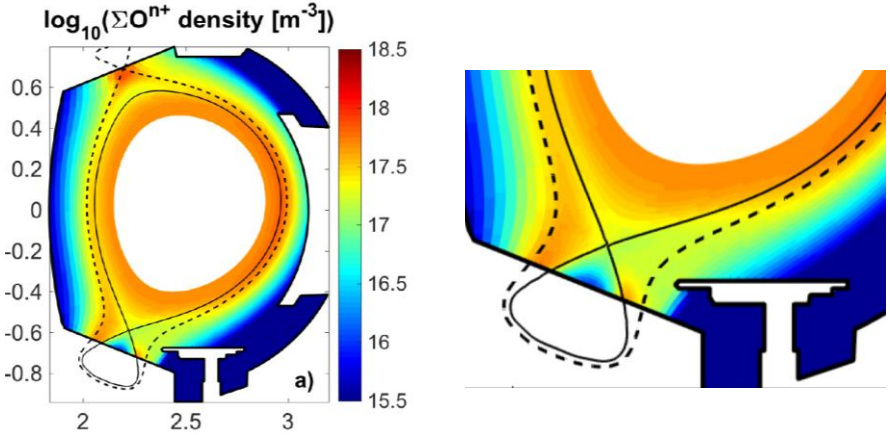

Maps of Oxygen concentration simulated with SOLEDGE3X-EIRENE showing inner-outer asymmetry.

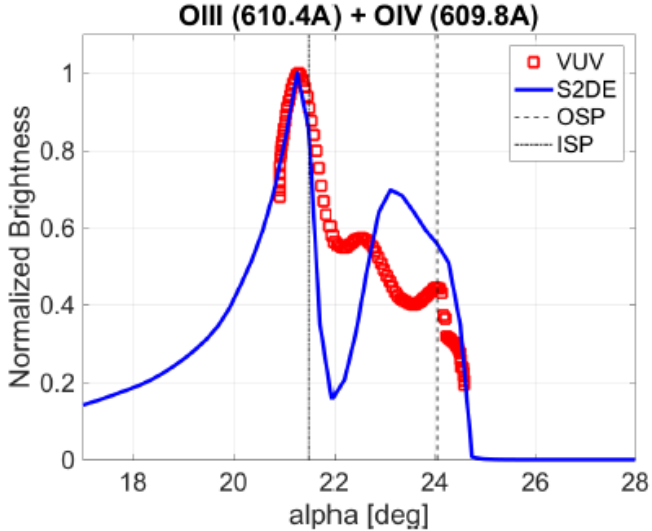

Comparison with VUV measurements (synthetic diagnostic)

SP4.4 Transport simulation: estimating W sources (CEA)

ERO2.0 simulations have been performed with SOLEDGE3X background plasmas to simulate W erosion and transport

- Purpose: understand W sputtering
  - Location
  - Intensity: erosion by D, light impurities, self sputtering
- First results: 2 WEST simulations, same power:
  - low density case $n_{sep} = 5 \cdot 10^{18} m^{-3}$
  - high density case $n_{sep} = 1 \cdot 10^{19} m^{-3}$

[**A. Gallo, A. Sepetys et al., Phys. Scripta T171, 2020**]

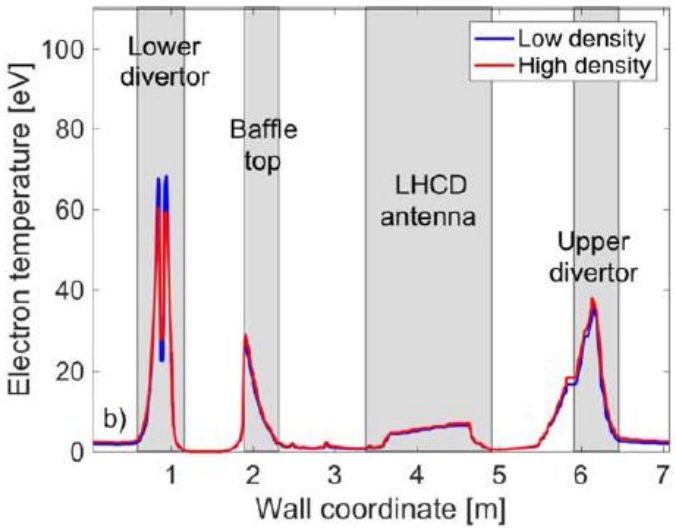

SP4.4 Transport simulation: estimating W sources (CEA)

ERO2.0 simulations have been performed with SOLEDGE3X background plasmas to simulate W erosion and transport

Maps of W density computed by ERO2.0. 1% concentration Oxygen is assumed. Reduction of W at high density can be explained by higher prompt redeposition and better screening.

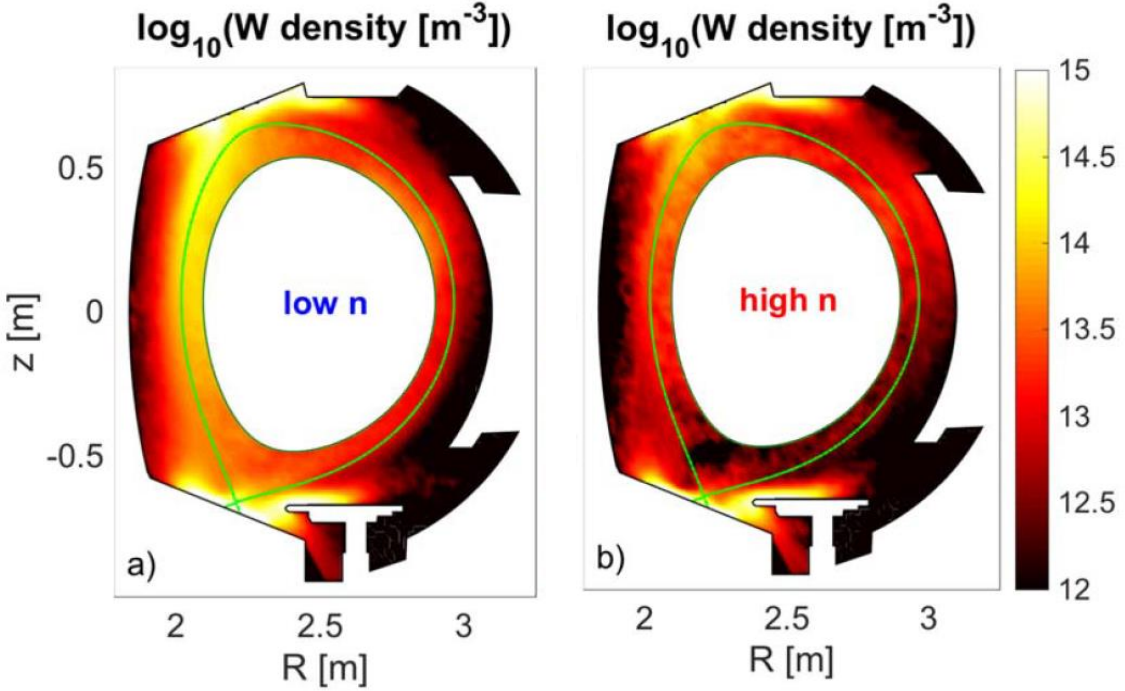

Work in progress: Account for sputtering made by a mixture of species (eg. O+N+W). Estimate the effect of puffing Nitrogen on W concentration.

SP4.4 Turbulent simulation (CEA)

SOLEDGE3X to simulate turbulent transport in the SOL

“First principle” turbulence simulation (ongoing):

- 3D simulations taking WEST wall geometry into account

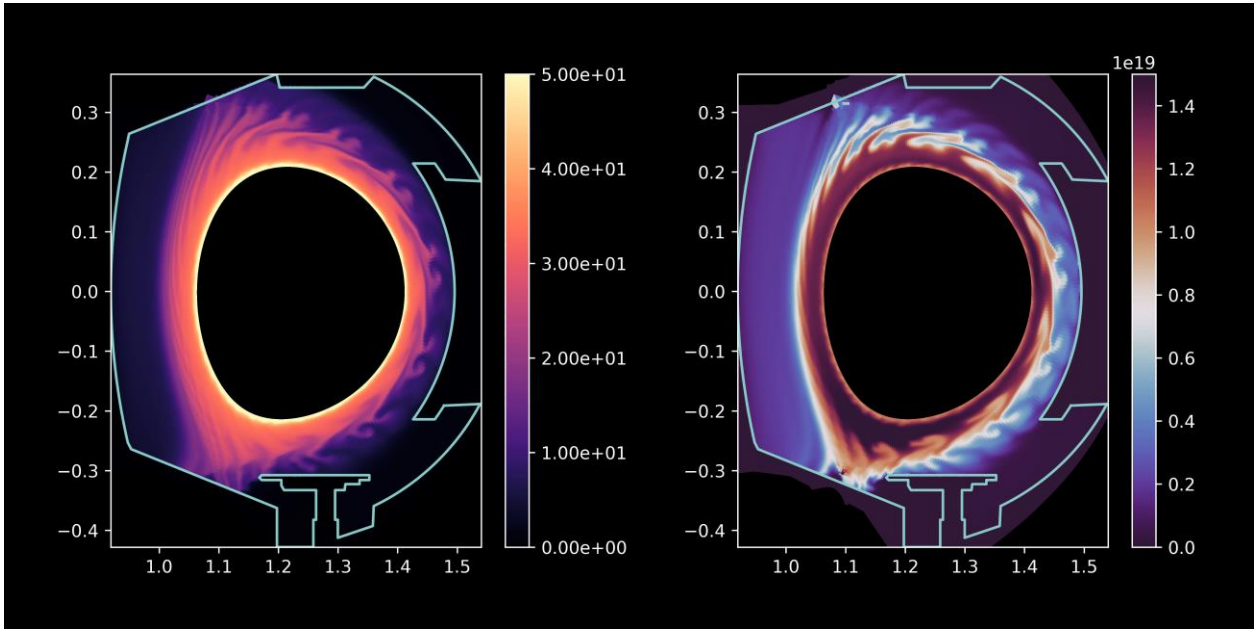

Turbulent simulation example (WEST scale ½).
Left: electron temperature – right: electron density

IPP.CR & VR tasks

M. Komm, R. Dejarnac, et al.
S. Ratynskaia et al.

SP4.4 Sheath modelling (IPP.CR & VR)

Development of state-of-the-art electron emission model:

- electron current emitted due to field-assisted thermionic emission in the extended Schottky regime
- energy distribution and angular distribution of the electrons that are ejected by field-assisted thermionic emission
- incident energy and angle dependence of the SEE, EBS yields of W
- energy distribution and angular distribution of the secondary and backscattered electrons

Implemented into PIC code SPICE 2D3V

SP4.4 Sheath modelling (IPP.CR & VR)

PIC results for the escaping thermionic current as function of surface temperature for ITER IVT ELM conditions.

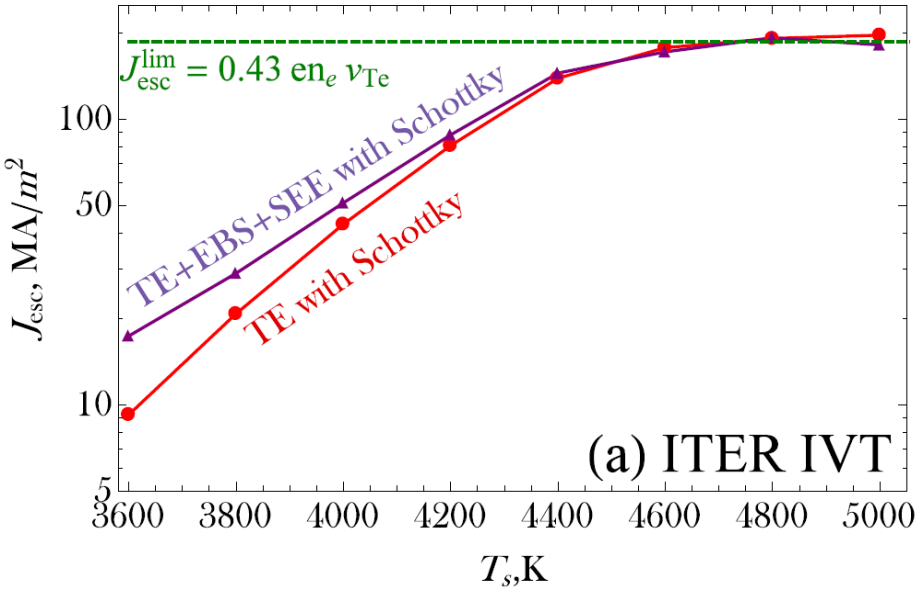

Importance of SEE+EBS

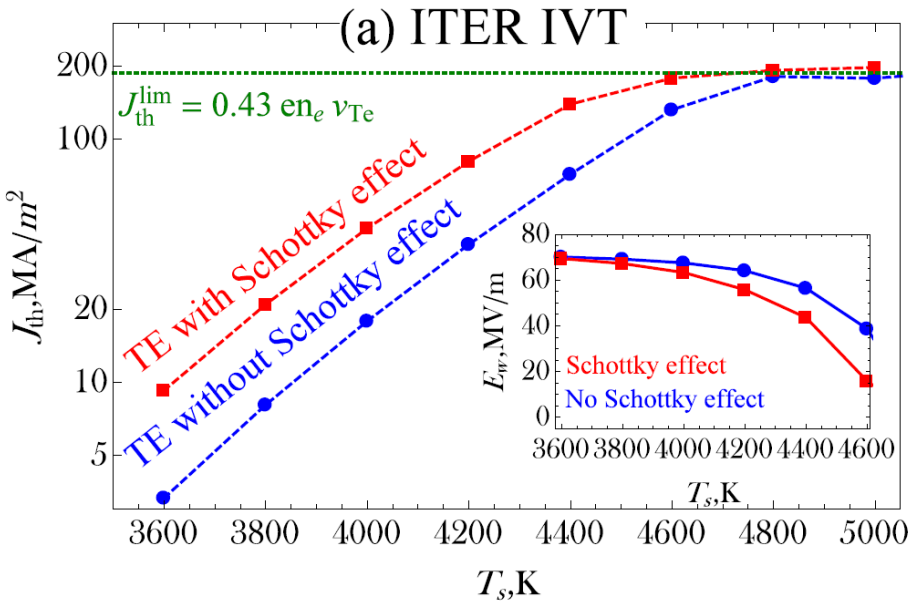

Importance of the Schottky effect

SP4.4 Sheath modelling (IPP.CR & VR)

Sheath characteristics at rough surfaces

Spatial scales:
a) $h < \lambda_D$: potential as with flat surface
b) $\lambda_D < h \leq r_{Li}$: scale of interest
c) $h >> r_{Li}$: potential follows surface

- The potential decay length in the Debye sheath does increase between the “summit” of the peak and the “valley”.
- In some studied cases this variation can be approximated by an exponential dependence

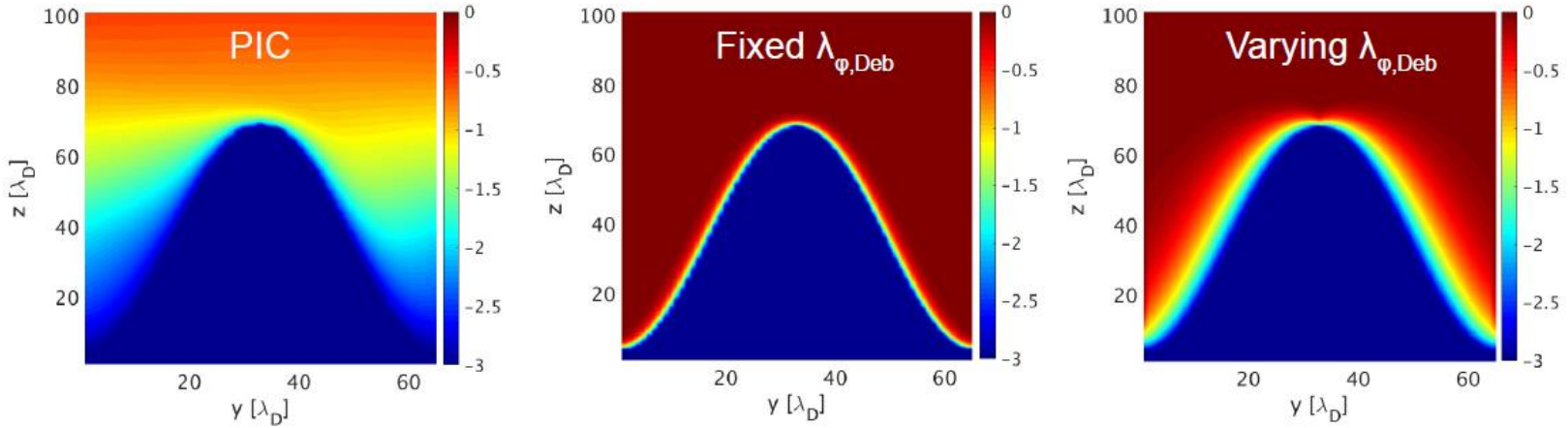

Report on WP JET2 SP3

Report on WP JET2 SP3

Most JET modelling tasks are included in WP JET1 / T17-12, however, some specific tasks are running under WP PFC (e.g. background plasma modelling for JET, retention/release modelling)

General aim of JET2 SP3:

ensure that post-mortem data are made available for modelling

Report on WP JET2 SP3

Modelling tasks related to JET2:

- Global erosion/deposition studies, WallDYN and ERO2.0
- Impurity migration to remote areas & gaps of JET
- Melt experiments (MEMOS)
- Fuel retention … dust modelling … (CRDS, …)

Post-mortem data of interest:

- Erosion/deposition on wall tiles, castellations, rotating collector probes, QMBs, Be-10 deposition, morphology measurements ...
- Data on fuel retention and dust

Thank you for your attention !